Supplementary Information (SI) for Journal of Materials Chemistry C.

Phenolic Deprotonation Triggered NIR-emission and Large Stokes Shift of BODIPY dyes

Ying Zou[a], Zhengrong Li[a], Huan Ma[a], Xinying Xu[a], ChunlaiYang[a], Yifu Huang[a,b], Hefeng Zhang*[a,b,c]

[a.] Department of Chemistry and Key Laboratory for Preparation and Application of Ordered Structural Materials of Guangdong Province, College of Chemistry and Chemical Engineering, Shantou University, Shantou, 515063, China.

[b.] GuangDong Engineering Technology Research Center of Advanced Polymer Synthesis, Shantou University, Shantou, 515063, China.

[c.] Chemistry and Chemical Engineering Guangdong Laboratory, Shantou 515031, China

* Corresponding author. Email: hfzhang@stu.edu.cn (Hefeng Zhang)

1. Experimental methods

Materials and Instruments

All chemicals and reagents were purchased from Energy-Chemical Company. Solvents were purified and dried by standard methods before use. The microwave reaction was conducted using a normal pressure microwave chemical reactor (MCR-3 type). UV-vis spectra were recorded on a UV-4802S (UNICO, Shanghai, China) UV-visible spectrophotometer. Fluorescence spectra were measured on a QM-TM (PTI, US) spectrophotometer. The absolute fluorescence quantum yield was determined by using a Hamamatsu quantum yield spectrometer C11347 Quantaurus-QY. Proton and carbon nuclear magnetic resonance spectra (^{1}H and ^{13}C NMR) were recorded on an AVANCE-400 MHz and 100 MHz NMR spectrometer, respectively, with TMS as an internal reference. Mass spectra were measured by High-Resolution Mass Spectrometry (HRMS) (Orbitrap Exploris 120, Thermo Fisher Scientific, US). Quantum computations were conducted by using the DFT method at B3LYP/6-311+G (d, p) levels.

2. Supplementary tables and figures

2.1 The absorption and emission spectra of HS-X-BODs.

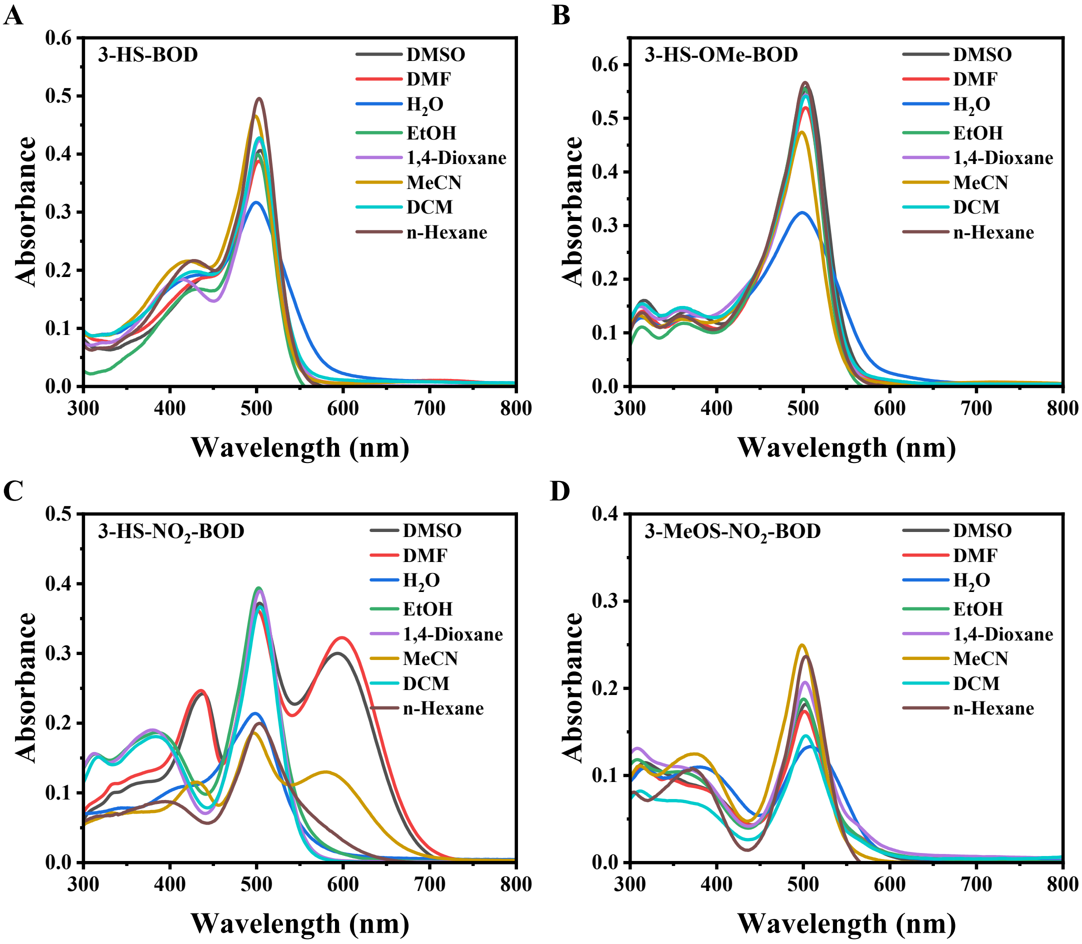

Figure S1. The absorption spectra of 3-HS-X-BODs and 3-MeOS-NO$_2$-BOD.

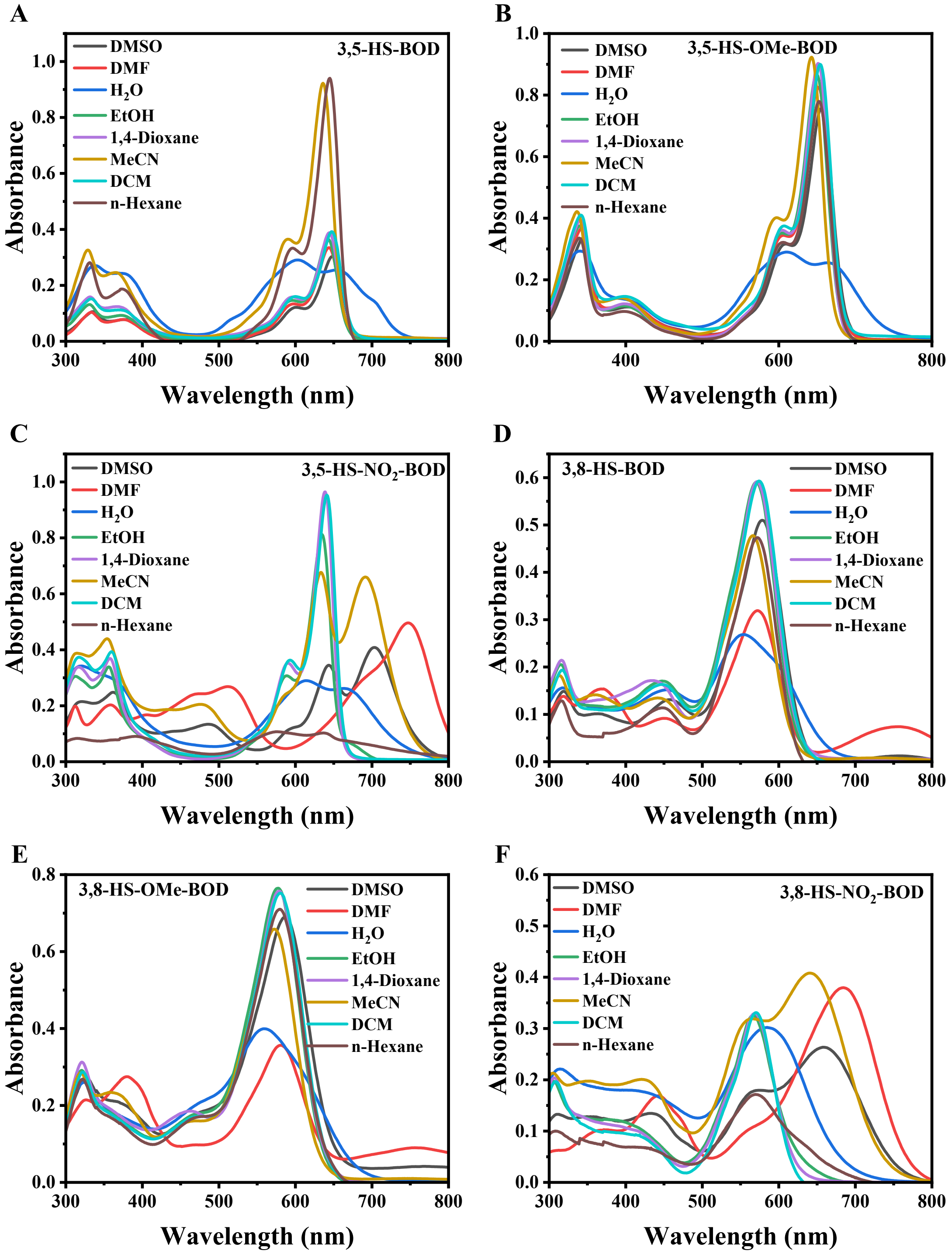

Figure S2. The absorption spectra of 3,5-HS-X-BODs and 3,8-HS-X-BODs.

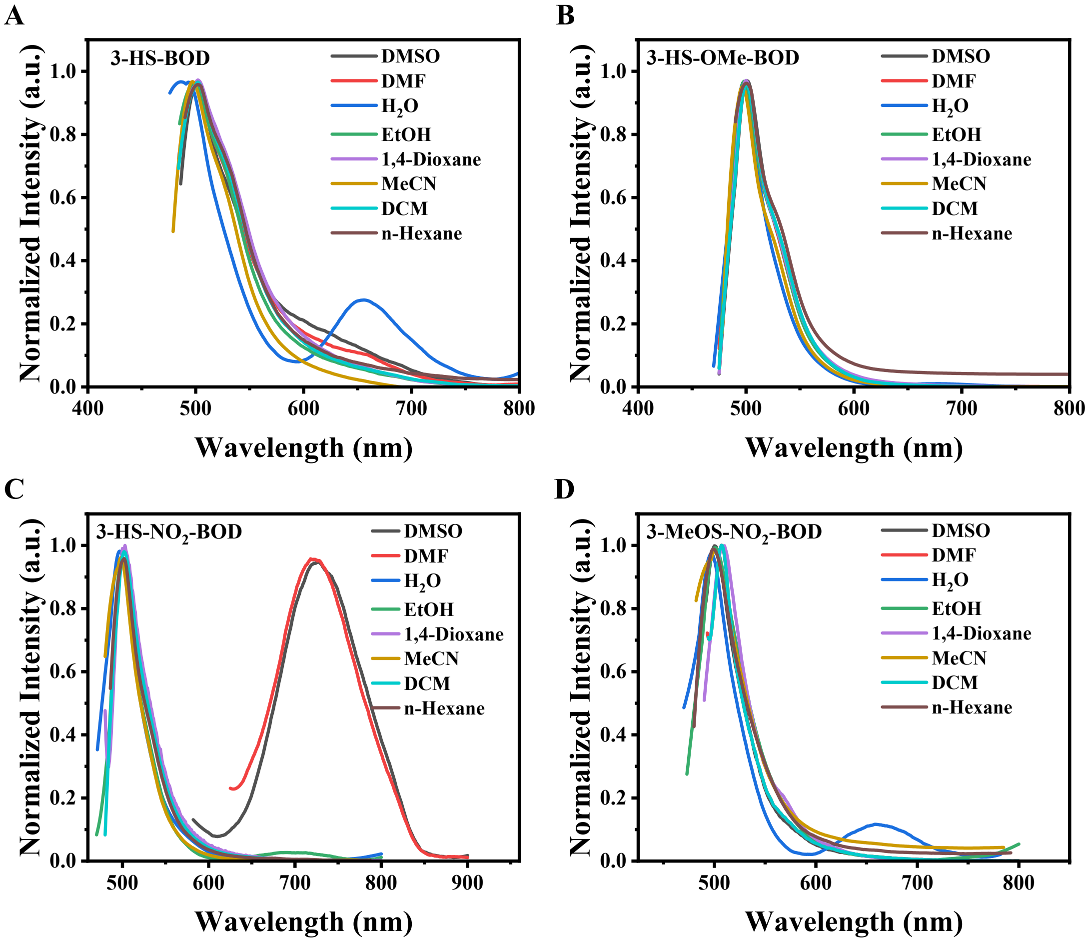

Figure S3. The emission spectra of 3-HS-X-BODs and 3-MeOS-NO$_2$-BOD.

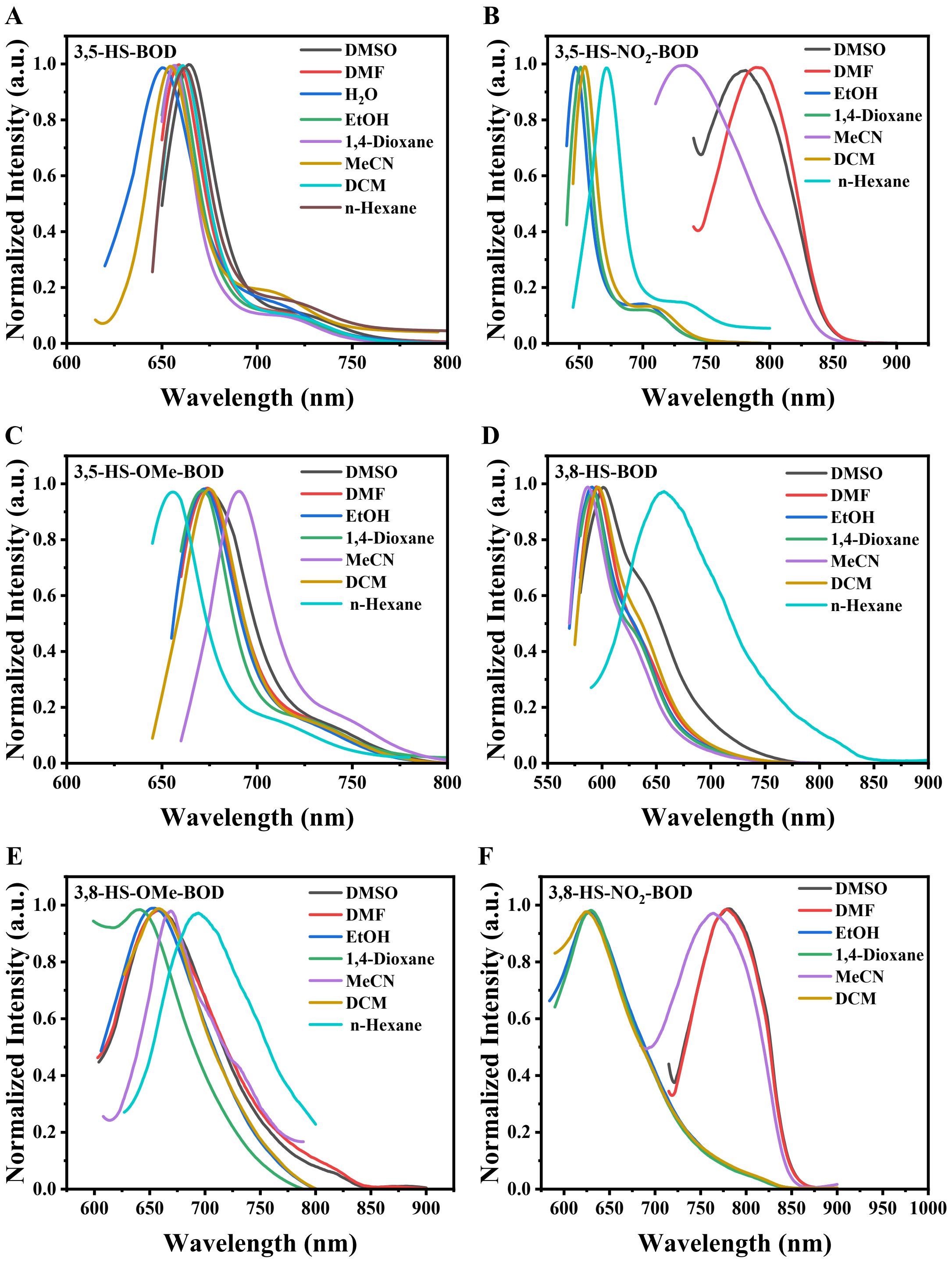

Figure S4 The emission spectra of 3,5-HS-X-BODs and 3,8-HS-X-BODs.

2.2 Absorption and emission spectra under the influence of acidity and alkalinity

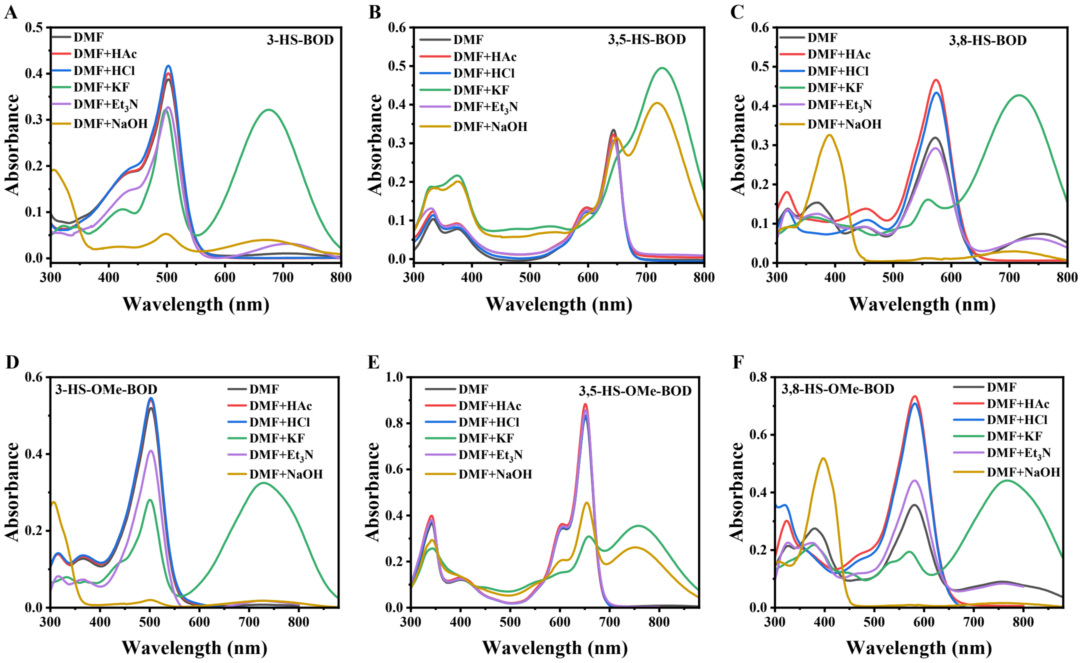

Figure S5. The absorption spectra of HS-X-BODs in DMF were affected by acid and base.

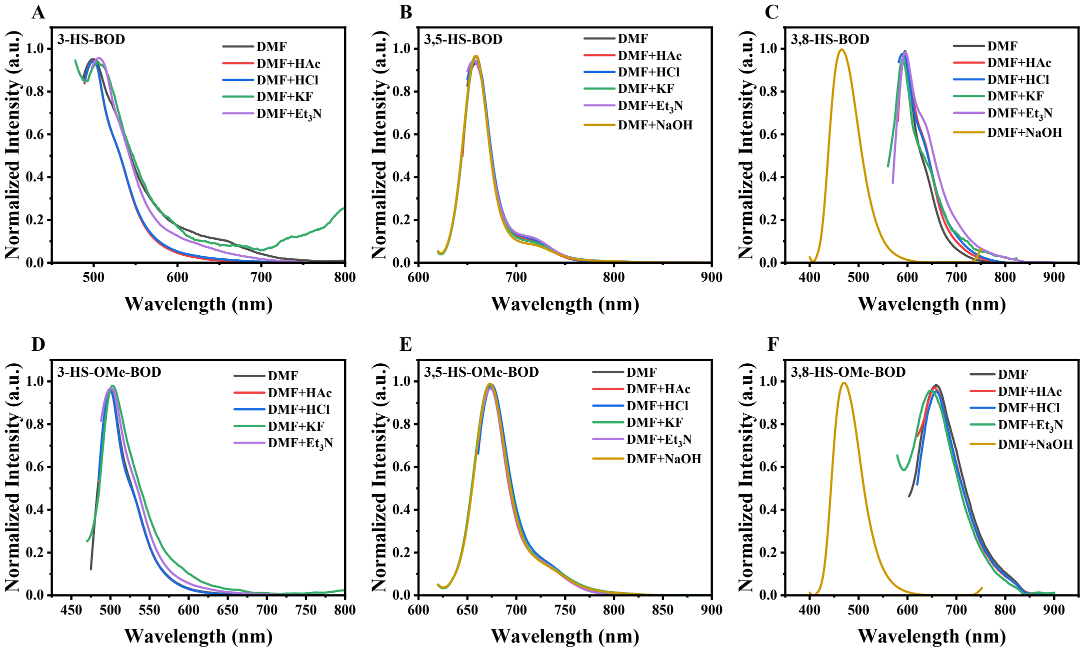

Figure S6. The emission spectra of HS-X-BODs in DMF were affected by acid and base.

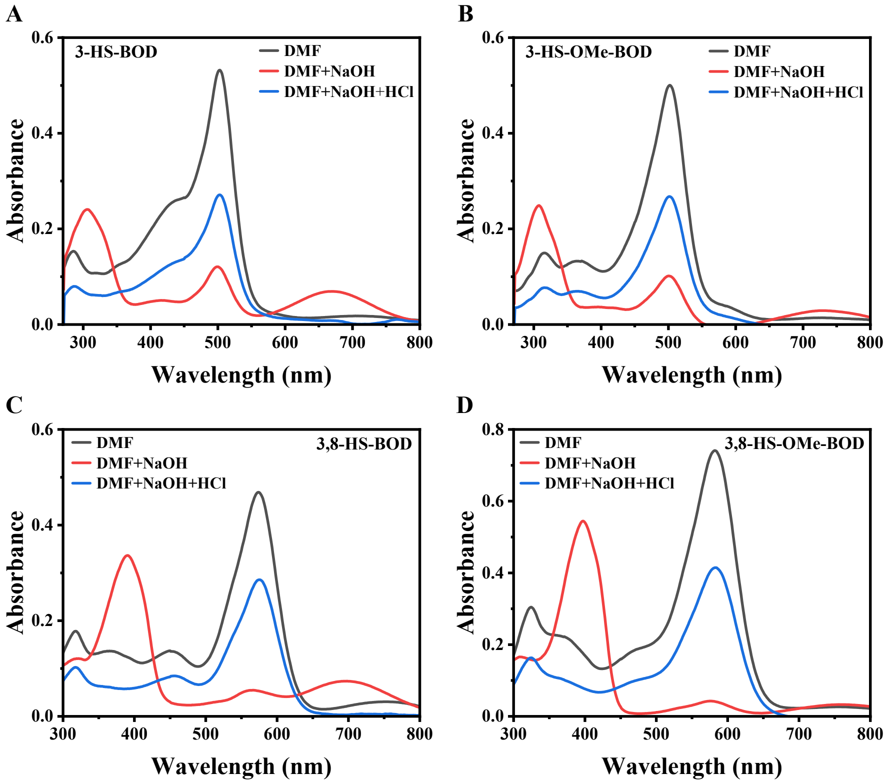

Figure S7. The absorption spectra of (A) 3-HS-BOD, (B) 3-HS-OMe-BOD, (C) 3,8-HS-BOD and (D) 3,8-HS-OMe-BOD in DMF solution, DMF (NaOH) solution, and DMF (NaOH) solution with added HCl.

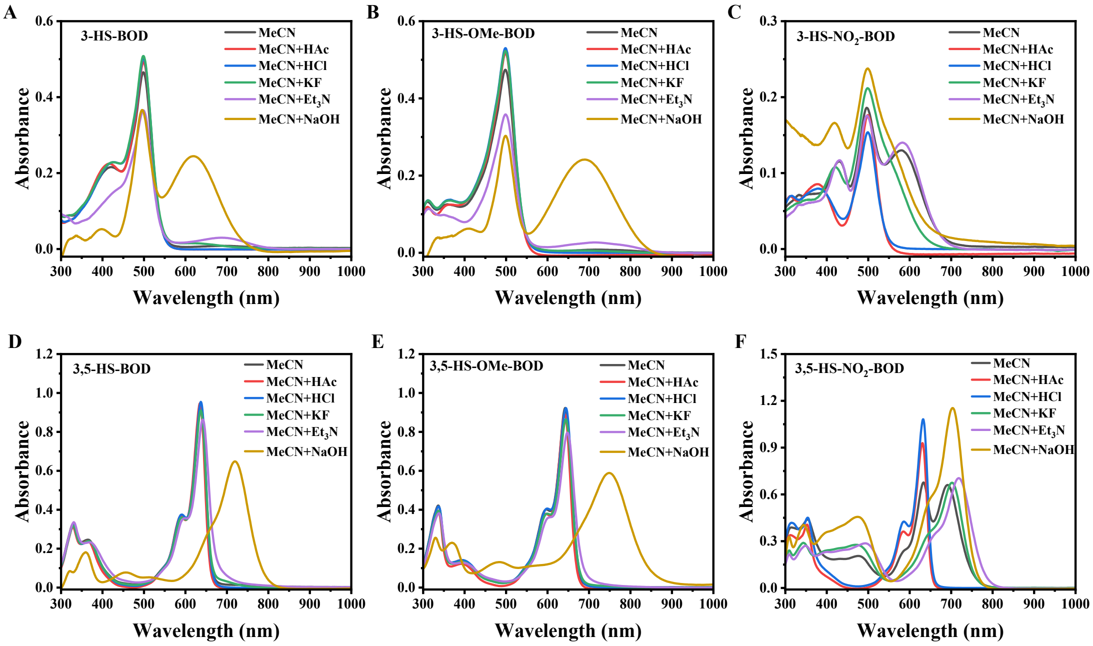

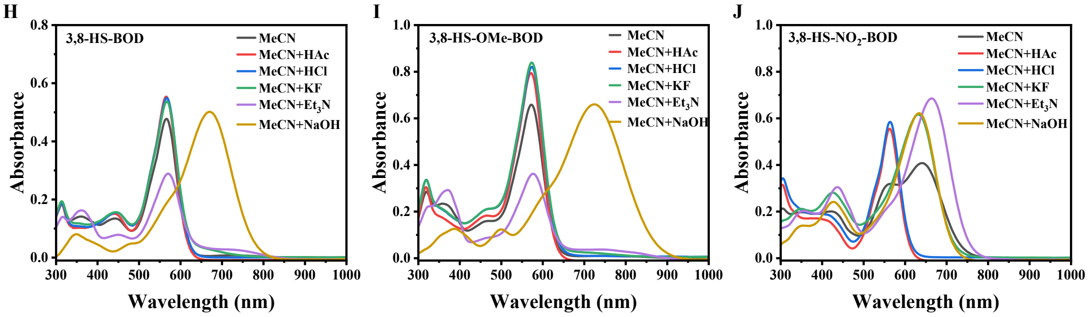

Figure S8. The absorption spectra of HS-X-BODs in MeCN were affected by acid and base.

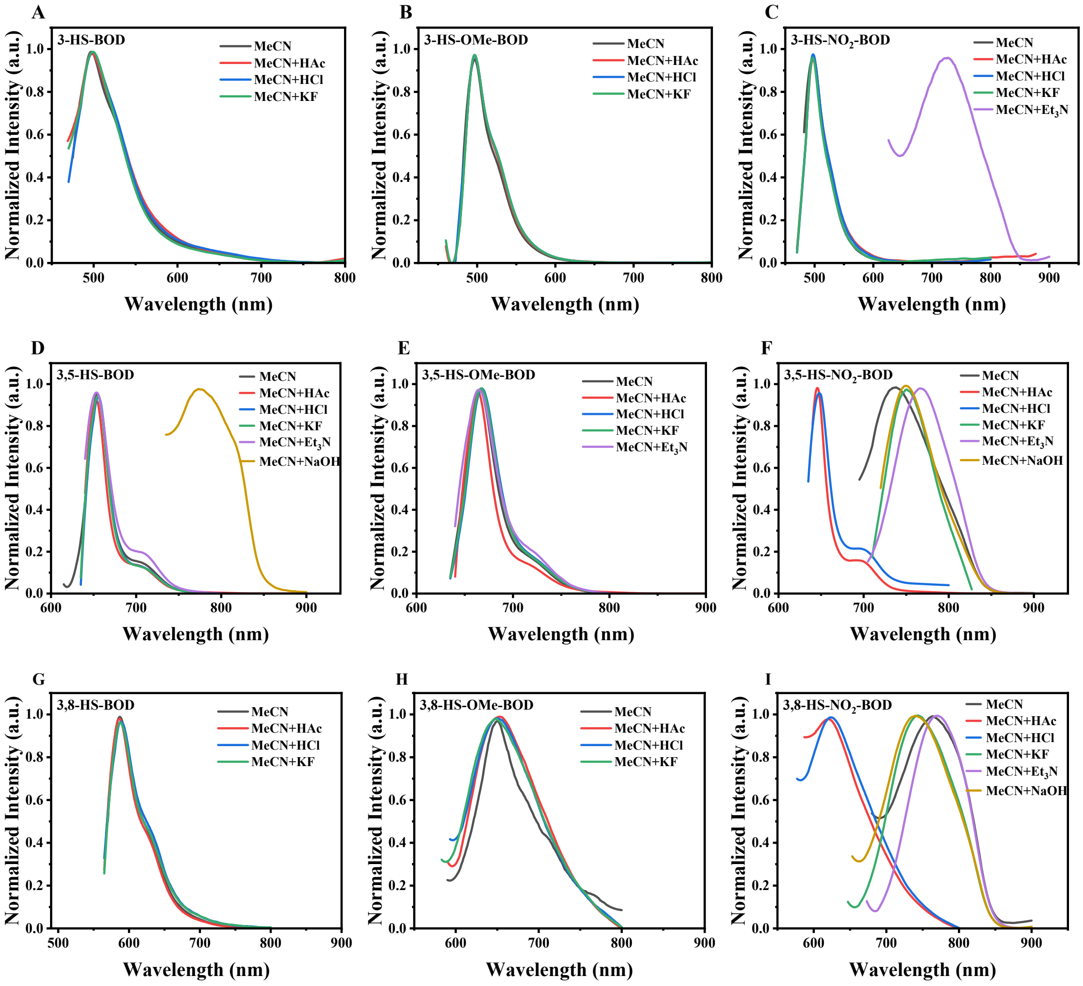

Figure S9. The emission spectra of HS-X-BODs in MeCN were affected by acid and base.

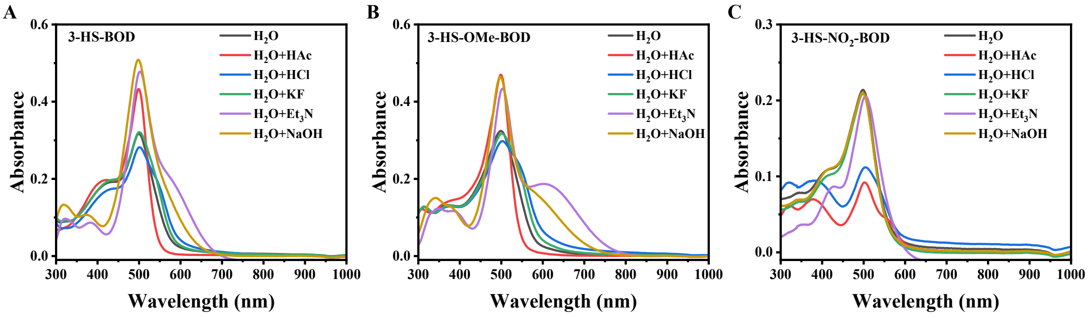

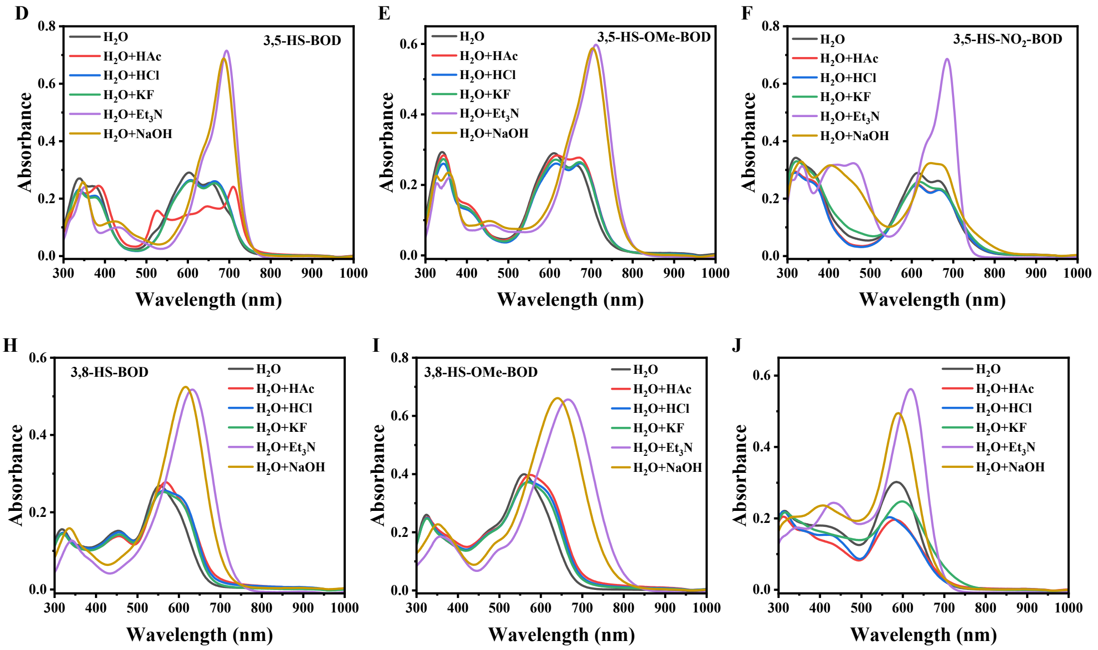

Figure S10. The absorption spectra of HS-X-BODs in H_2O were affected by acid and base.

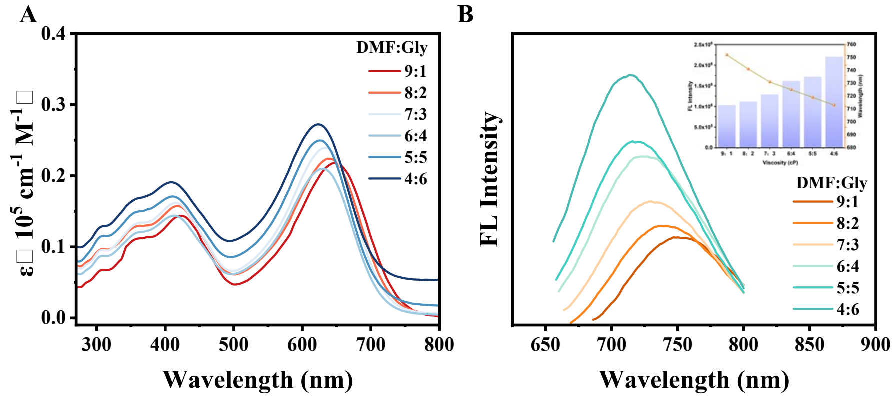

Figure S11. The absorption and emission spectra of 3,8-HS-NO_2-BOD in DMF solutions contain varying glycerol proportions.

2.3 Photostability Evaluation of HS-NO_2-BODs.

HS-NO_2-BODs were dissolved in DMSO to prepare a 0.01 mM solution and placed in a quartz cuvette with four transparent sides. Subsequently, the solution was irradiated under laser beams of different wavelengths (1W/cm²) for 20 minutes. The absorbance of the solution was measured every 2 minutes using an ultraviolet spectrophotometer. Absorption spectra were measured using a UV–vis spectrophotometer at room temperature with a 1 cm quartz cuvette. To demonstrate the good photostability of HS-NO_2-BODs, the photostability of 3,5-dimethyl BODIPY and 3,8-dimethyl BODIPY was also evaluated.

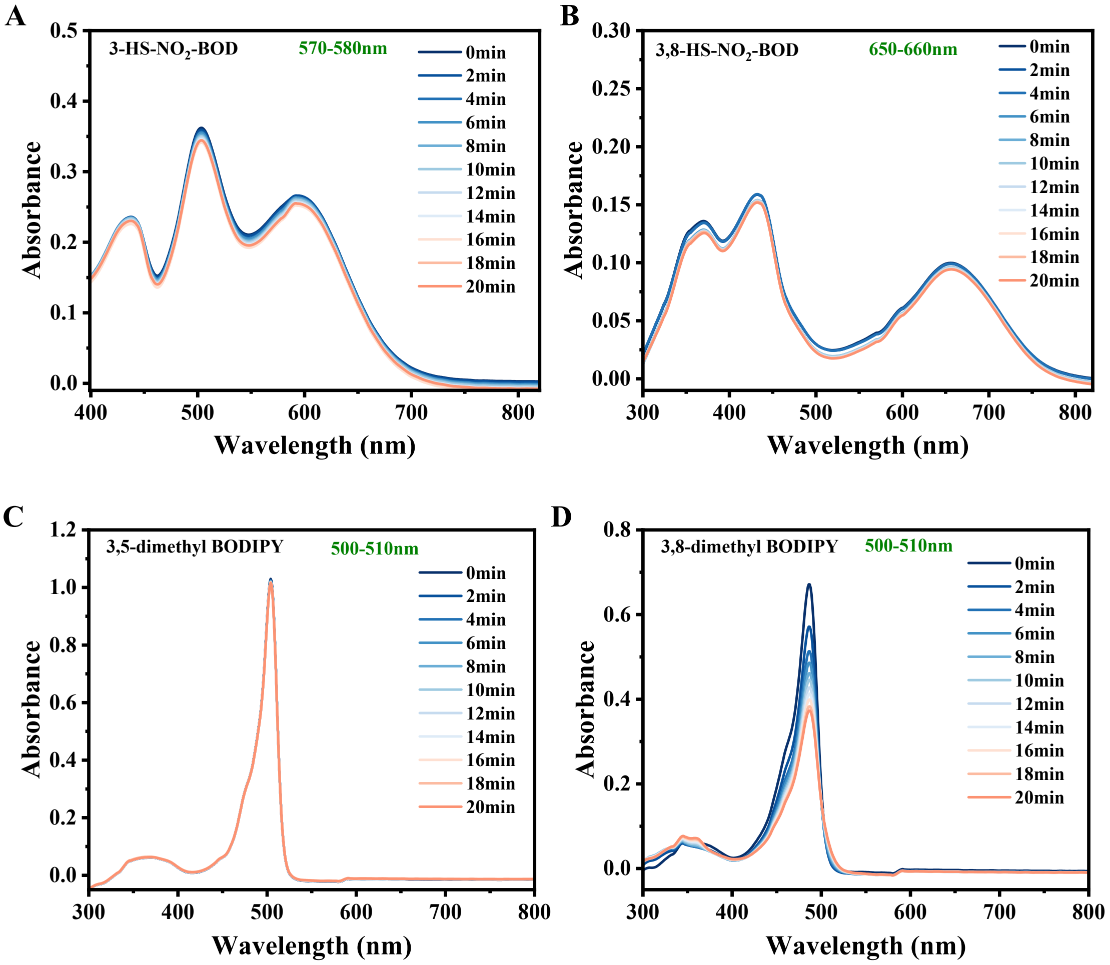

Figure S12. Absorption spectra of the (A)3-HS-NO_2-BOD, (B) 3,8-HS-NO_2-BOD, (C) 3,5-dimethyl BODIPY and (D) 3,8-dimethyl BODIPY for photodegradation studies in DMSO under the light source.

Measurement of singlet oxygen ($^1O_2$) generation ability of HS-X-BODs.

In a dark environment, HS-X-BODs (1 mM) were added to a solution of DPBF (0.04 mM) in DMSO (2 mL). The photosensitizer was irradiated with LED lasers ($1W/cm^2$) of different excitation wavelengths, and their absorbance spectra were recorded every 2 minutes to evaluate their photodynamic effect. Additionally, DPBF (0.04 mM) in DMSO solution was irradiated at the wavelengths of 500-510 nm, 570-580 nm, 650-660 nm, and 680-690 nm for the same duration to demonstrate that the degradation of DPBF is due to singlet oxygen generated by the photosensitizer, rather than photodegradation.

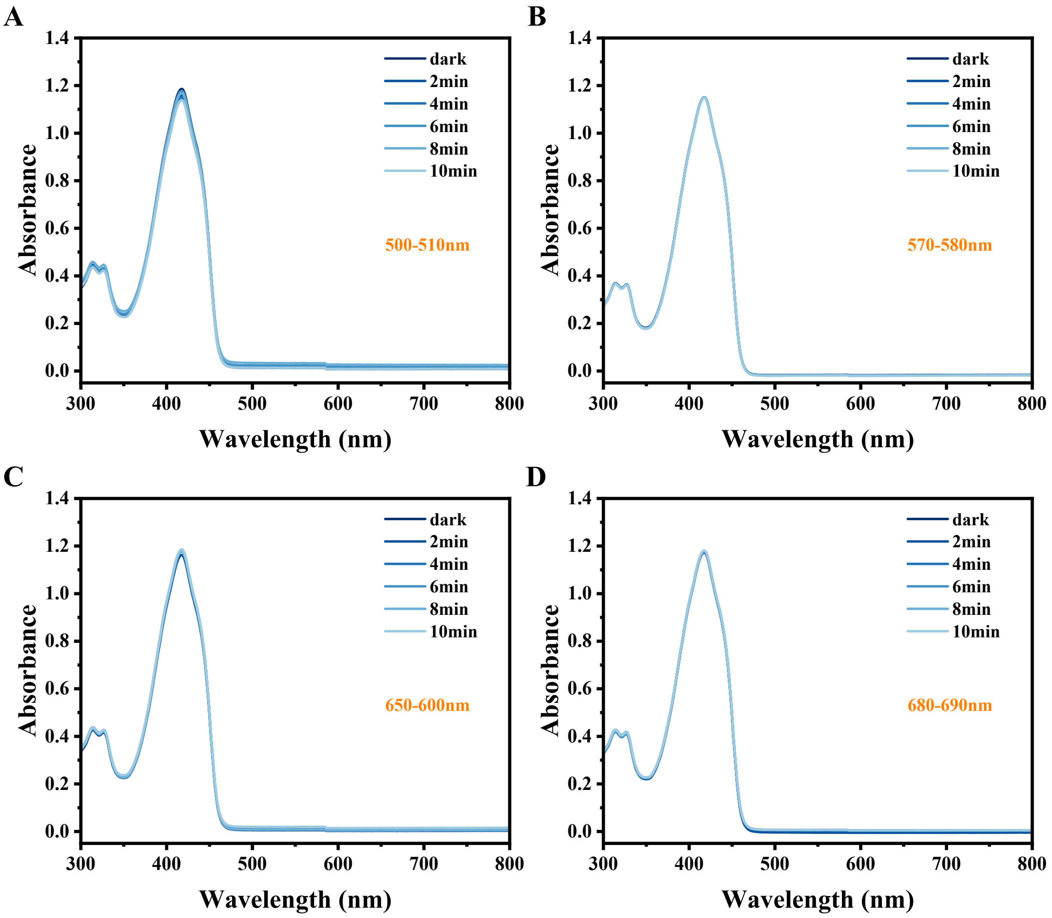

Figure S13. Absorbance spectra of DPBF under LED ($1W/cm^2$) irradiation at different wavelengths in DMSO ($c = 0.04$ mM).

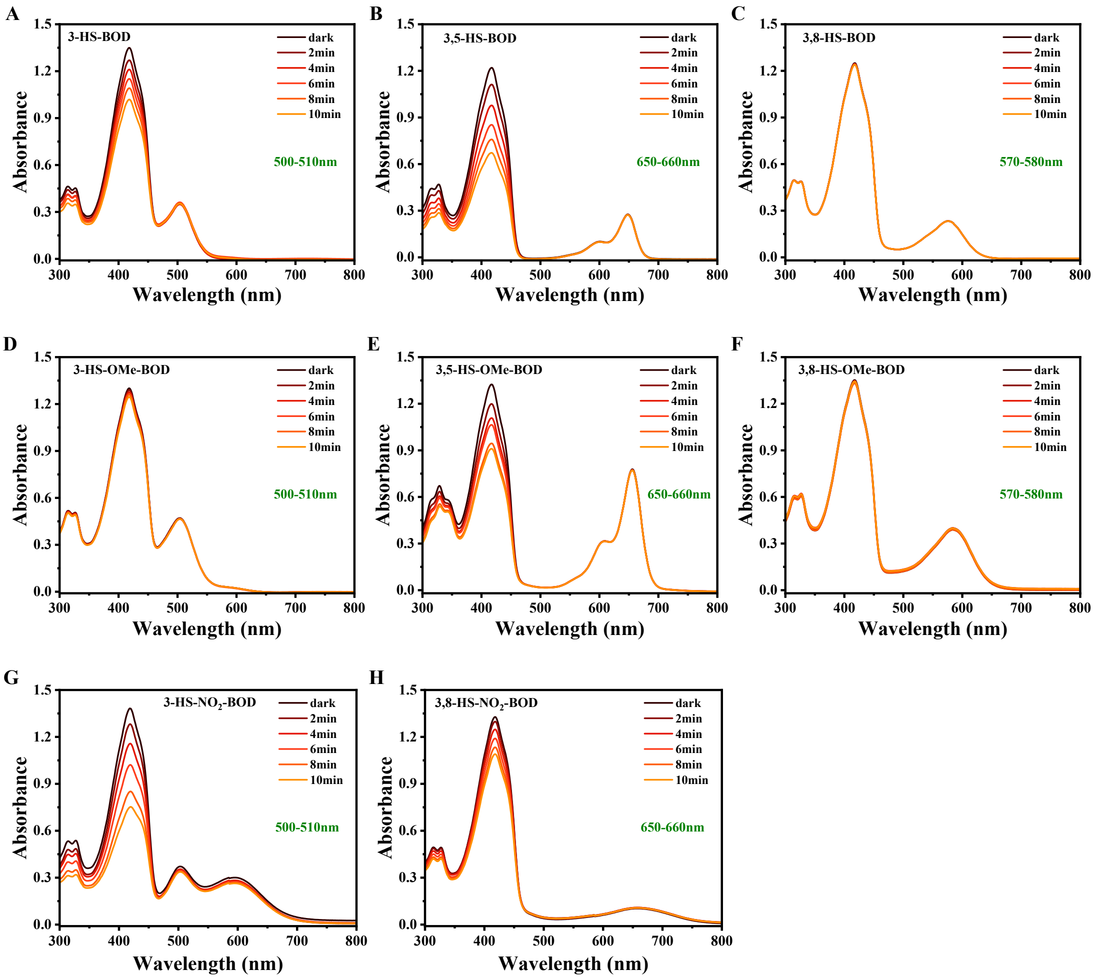

Figure S14. Absorbance spectra of HS-X-BODs under LED (1W/cm^2) irradiation at different wavelengths in DMSO (c = 0.01 mM).

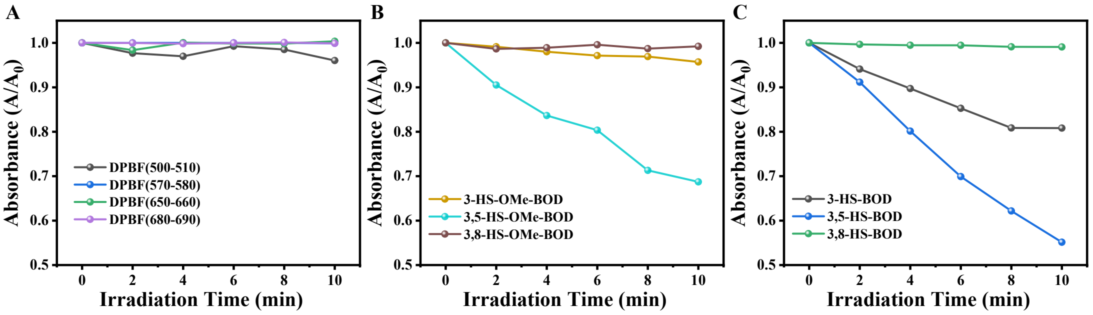

Figure S15. The decrease in the absorbance band of trap molecule (DPBF) (0.04 mM) in the presence of HS-BODs and HS-OMe-BODs (c = 0.01 mM) in DMSO.

Penetration depth evaluation in tissue phantom imaging

To study the penetration depth of HS-NO_2-BODs during fluorescence imaging, fresh pork tenderloin purchased from a local market was used as a biological tissue model and was cut into different thicknesses for this purpose. A 1 mM solution of HS-NO_2-BODs in DMSO was prepared and injected into a glass capillary tube (0.3*100mm). The glass capillary tube was then placed under an infrared camera. Excitation light sources with wavelengths of 570-580 nm (for 3-HS-NO_2-BOD), 650-660 nm (for 3,5-HS-NO_2-BOD), and 680-690 nm (for 3,8-HS-NO_2-BOD) were used, along with long-pass filters of 700-900 nm (for 3,5-HS-NO_2-BOD) and 750-800 nm (for 3,5-HS-NO_2-BOD and 3,8-HS-NO_2-BOD) for fluorescence imaging. The NIR fluorescence penetration depth of HS-NO_2-BODs was evaluated by covering the glass capillary tube with varying thicknesses of pork.

3. Density functional theory (DFT) calculations

The ground states of all structures were optimized at the B3LYP/6-311G+(d, p) level. The time-dependent density functional theory (TD-DFT) calculation used the B3LYP/6-311+G (d, p) method based on their optimized S_0 geometries. All the calculations were performed in Gaussian 09.

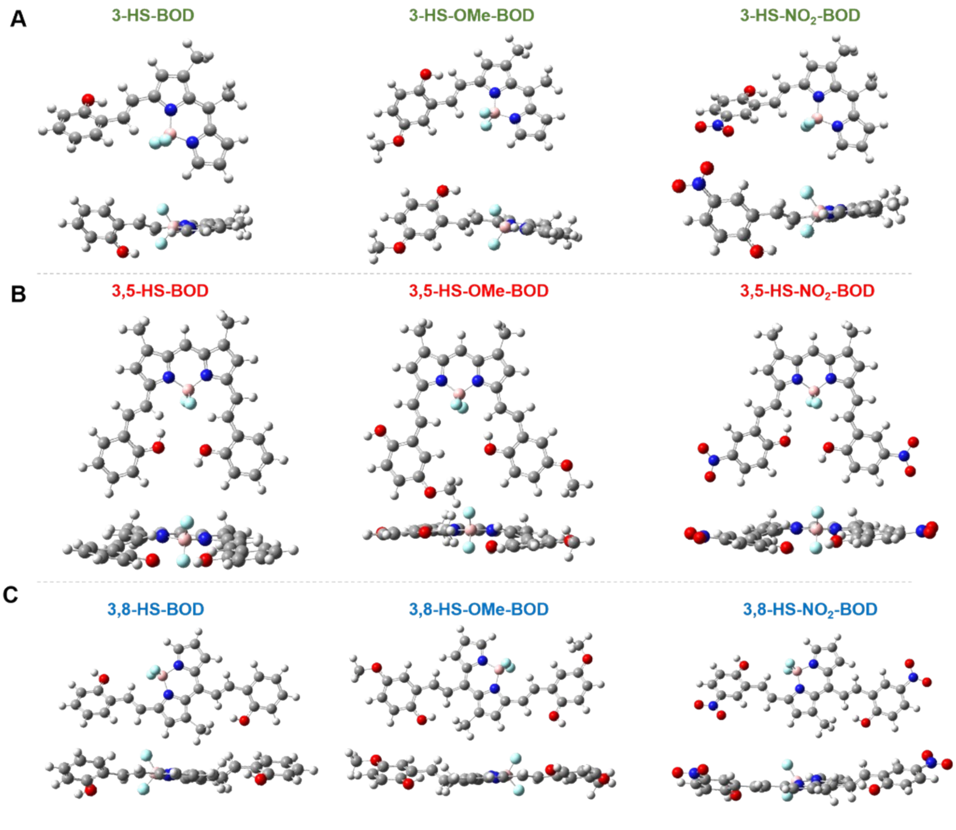

Figure S16. Skeleton structures of HS-X-BOD dyes in the ground state (S_0).

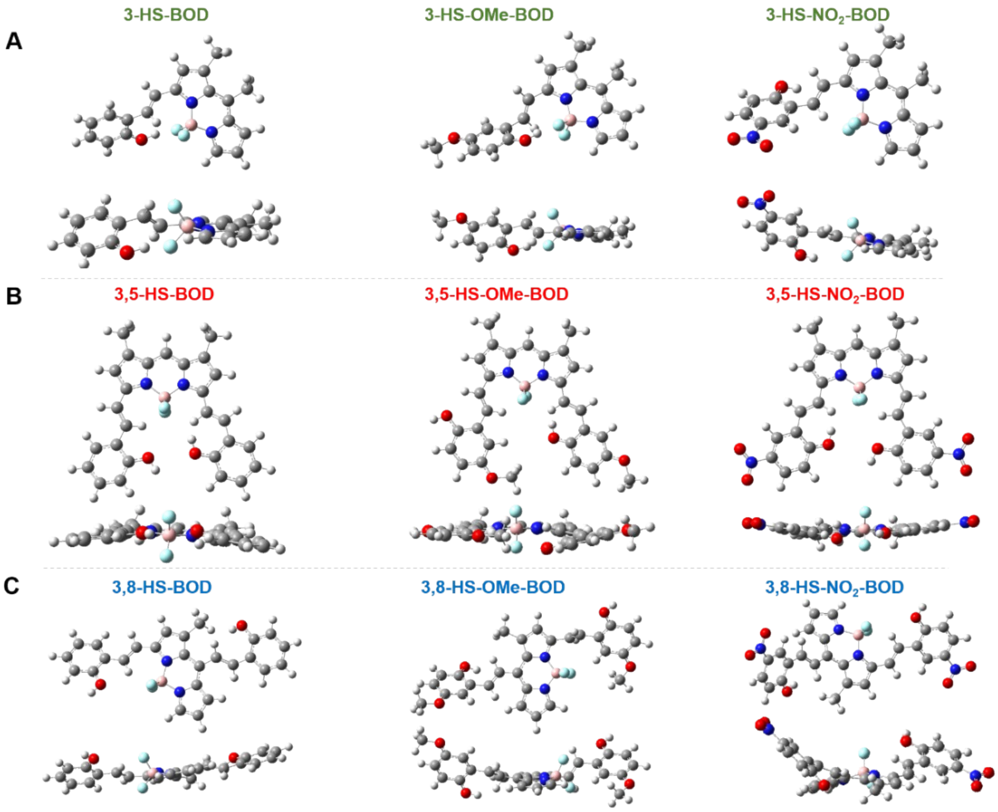

Figure S17. Skeleton structures of HS-X-BOD dyes in the excited state (S_1).

Table S1. Photophysical properties of 3-HS-X-BODs derivatives in solutions.

Sample	**Solvent**[a]	λ_{abs} **(nm)**	ε[b] **($M^{-1}\cdot cm^{-1}$) $*10^5$**	λ_{ex} **(nm)**	λ_{em} **(nm)**	**Stokes shift (nm)**	**QY**[d] **(%)**
3-HS-BOD	DMSO	504	0.4061	485	503	-[c]	0.60
	DMF	503	0.3876	485	498	-[c]	0.40
	EtOH	501	0.3992	483	499	-[c]	0.80
	Dioxane	503	0.4232	486	503	-[c]	1.00
	MeCN	498	0.4654	480	498	-[c]	0.50
	H_2O	499	0.3166	480	495	-[c]	1.10
	n-Hexane	503	0.4949	488	503	-[c]	0.60
	DCM	503	0.4279	486	503	-[c]	0.70
3-HS-OMe-BOD	DMSO	503	0.5579	484	502	-[c]	0.60
	DMF	501	0.5197	482	499	-[c]	0.50
	EtOH	501	0.5552	483	499	-[c]	0.90
	Dioxane	502	0.5436	485	501	-[c]	1.00
	MeCN	498	0.3241	477	501	-[c]	0.60
	H_2O	498	0.4742	480	498	-[c]	0.80
	n-Hexane	502	0.5411	487	501	-[c]	0.70
	DCM	502	0.5411	485	501	-[c]	0.80
3-HS-NO_2-BOD	DMSO	505/595	0.3720	597	727	222	1.30
	DMF	501/598	0.3607	601	726	225	1.10
	EtOH	502	0.3939	500	501	-[c]	4.00
	Dioxane	502	0.3892	479	504	2	1.30
	MeCN	501/581	0.3000	479	500	-[c]	0.80
	H_2O	498	0.2134	495	498	-[c]	1.30
	n-Hexane	503	0.1997	486	503	-[c]	0.90
	DCM	504	0.3668	494	503	-[c]	0.90
3-MeOS-BOD	DMSO	502	0.1816	484	502	-	0.80
	DMF	501	0.1734	487	5077	7	0.15
	EtOH	500	0.1876	489	502	-[c]	1.60
	Dioxane	501	0.2068	489	510	9	5.30
	MeCN	498	0.2496	480	501	3	0.80
	H_2O	508	0.1331	485	498	-[c]	1.00
	n-Hexane	502	0.2363	491	500	-[c]	0.60
	DCM	501	0.1456	487	508	7	3.20

a. Samples were dissolved in solvents with a concentration of 10^{-5} M; b. Molar extinction coefficients (ε) were measured with excitation at the absorption maximum. c. The absorption and emission wavelengths overlap severely and cannot be calulated. d. Absolute photoluminescence quantum yields (QY) of dyes in solution were determined by using the integrating sphere method.

Table S2. Photophysical properties of 3,5-HS-X-BODs derivatives in solutions.

Sample	Solvent[a]	λ_{abs} (nm)	ε^b ($M^{-1}\cdot cm^{-1}$) *10^5	λ_{ex} (nm)	λ_{em} (nm)	Stokes shift (nm)	QY[c] (%)
3,5-HS-BOD	DMSO	648	0.3031	649	665	17	51.00
	DMF	644	0.3348	645	659	15	52.20
	EtOH	643	0.3646	642	658	15	43.40
	Dioxane	644	0.3882	644	656	12	50.00
	MeCN	636	0.9225	634	655	19	44.20
	H_2O	602/657	0.2906/0.2544	640	651	49	0.50
	n-Hexane	645	0.9401	646	662	17	45.40
	DCM	648	0.3917	648	665	14	27.40
3,5-HS-OMe-BOD	DMSO	656	0.7564	653	678	22	12.60
	DMF	651	0.8250	651	674	23	18.00
	EtOH	649	0.8672	651	673	24	29.50
	Dioxane	651	0.9030	643	670	19	41.10
	MeCN	644	0.9198	650	690	46	15.40
	H_2O	611/667	0.2900/0.2548	Nd	Nd	Nd	0.40
	n-Hexane	652	0.7793	652	656	4	3.80
	DCM	654	0.8998	651	675	21	37.50
3,5-HS-NO_2-BOD	DMSO	706	0.4084	740	781	75	6.60
	DMF	747	0.4962	740	791	44	6.80
	EtOH	635	0.8125	633	647	12	14.00
	Dioxane	639	0.9643	637	651	12	31.2
	MeCN	633/690	0.6766/0.6601	690	732	102	4.30
	H_2O	613/663	0.2895/0.2619	Nd	Nd	Nd	0.40
	n-Hexane	579/637	0.1068/0.1025	636	672	93	10.70
	DCM	641	0.9528	640	654	13	50.70

a. Samples were dissolved in solvents with a concentration of 10^{-5} M; b. Molar extinction coefficients (ε) were measured with excitation at the absorption maximum. c. Absolute photoluminescence quantum yields (QY) of dyes in solution were determined by using the integrating sphere method. Nd: not detected.

Table S3. Photophysical properties of 3,5-HS-X-BODs derivatives in solutions.

Sample	Solvent[a]	λ_{abs} (nm)	ε[b] ($M^{-1}\cdot cm^{-1}$) $*10^5$	λ_{ex} (nm)	λ_{em} (nm)	Stokes shift (nm)	QY[c] (%)
3,8-HS-BOD	DMSO	579	0.5098	574	603	24	1.60
	DMF	573	0.3189	572	594	21	1.40
	EtOH	571	0.5902	568	590	19	1.20
	Dioxane	572	0.5917	571	591	19	1.40
	MeCN	565	0.4775	563	587	22	1.20
	H_2O	552	0.2683	Nd	Nd	Nd	0.70
	n-Hexane	573	0.4729	569	656	83	2.60
	DCM	574	0.5929	572	595	21	1.30
3,8-HS-OMe-BOD	DMSO	585	0.6888	561	658	73	0.40
	DMF	581	0.3564	565	657	76	0.30
	EtOH	577	0.7647	586	655	78	0.90
	Dioxane	579	0.7570	573	641	62	0.90
	MeCN	573	0.6583	575	669	96	0.40
	H_2O	562	0.3976	Nd	Nd	Nd	0.50
	n-Hexane	579	0.7098	579	691	112	0.80
	DCM	580	0.7920	607	657	77	0.70
3,8-HS-NO_2-BOD	DMSO	658	0.2635	697	782	124	1.40
	DMF	684	0.3796	697	780	96	2.40
	EtOH	566	0.3255	555	629	63	0.82
	Dioxane	568	0.3296	548	631	63	0.77
	MeCN	641	0.4080	685	766	125	0.60
	H_2O	587	0.3015	Nd	Nd	Nd	0.40
	n-Hexane	570	0.1714	Nd	Nd	Nd	0.80
	DCM	570	0.3310	551	624	54	0.59

a. Samples were dissolved in solvents with a concentration of 10^{-5} M; b. Molar extinction coefficients (ε) were measured with excitation at the absorption maximum. c. Absolute photoluminescence quantum yields (QY) of dyes in solution were determined by using the integrating sphere method. Nd: not detected.

Table S4. The fluorescence quantum yields of HS-X-BOD dyes in different environments.

Sample	**DMF**	**DMF+HAc**	**DMF+KF**	**DMF+Glycerol**
3-HS-BOD	0.4%	0.6%	0.4%	1.7%
3-HS-OMe-BOD	0.5%	0.5%	0.3%	2.1%
3-HS-NO_2-BOD	1.1%	0.7%	0.4%	2.8%
3,5-HS-BOD	52.2%	47.8%	0.3%	42.2%
3,5-HS-OMe-BOD	18.0%	18.5%	0.3%	18.1%
3,5-HS-NO_2-BOD	6.8%	45.4%	8.5%	5.2%
3,8-HS-BOD	1.4%	1.5%	0.3%	6.0%
3,8-HS-OMe-BOD	0.4%	0.4%	0.1%	1.4%
3,8-HS-NO_2-BOD	2.4%	0.9%	2.1%	2.5%

Table S5. O-H bond length and C-O bond length of HS-X-BODs.

Compound	Bond length (Å)			
	Ground state (S_0)		Excited state (S_1)	
	O-H	C-O	O-H	C-O
3-HS-BOD	0.966	1.364	1.027	1.291
3-HS-OMe-BOD	0.965	1.368	1.012	1.299
3-HS-NO_2-BOD	0.968	1.354	0.968	1.350
3,5-HS-BOD	0.968/0.963	1.362/1.356	0.964/0.967	1.355/1.360
3,5-HS-OMe-BOD	0.967/0.963	1.370/1.369	0.964/0.967	1.367/1.359
3,5-HS-NO_2-BOD	0.968/0.963	1.352/1.350	0.964/0.967	1.349/1.353
3,8-HS-BOD	0.964/0.962	1.365/1.361	0.964/0.963	1.355/1.368
3,8-HS-OMe-BOD	0.963/0.963	1.372/1.370	0.967/0.966	1.328/1.373
3,8-HS-NO_2-BOD	0.965/0.963	1.355/1.352	0.964/0.967	1.349/1.356

Table S6. Performing hole-electron analysis of HS-X-BOD dyes in excited states.

	Sm[a] (a.u.)	S_r[b] (a.u.)	Δσ[c] (Angstrom)	t index[d] (Angstrom)	D index[e] (Angstrom)	H index[f] (Angstrom)
3-HS-BOD	0.52117	0.77530	-0.097	-2.193	1.085	3.805
3,5-HS-BOD	0.55426	0.77884	-0.073	-2.294	0.502	4.294
3,8-HS-BOD	0.51626	0.78243	0.079	-1.748	1.948	4.199
3-HS-OMe-BOD	0.43586	0.72329	-0.370	-1.245	2.196	3.949
3,5-HS-OMe-BOD	0.52094	0.76568	-0.310	-1.985	0.909	4.367
3,8-HS-OMe-BOD	0.45264	0.74283	-0.311	-1.036	2.820	4.352
3-HS-NO_2-BOD	0.42524	0.71706	-0.050	-1.513	2.052	4.104
3,5-HS-NO_2-BOD	0.48593	0.75566	-0.254	-2.052	0.897	4.797
3,8-HS-NO_2-BOD	0.43028	0.73309	-0.326	-1.996	2.591	5.006

[a-b] Sm and Sr: a function representing the overlap between the distributions of electrons and holes. [c] Δσ index: the difference in the overall spatial distribution breadth between electrons and holes; [d] t-index: a measure of the degree of separation between holes and electrons; [e] D index: the distance between the centroids of holes and electrons.; [f] H index: the overall average spatial distribution breadth of electrons and holes.

4. Syntheses and characterization

4.1 Synthesis of compound of 3,5-dimethyl BODIPY

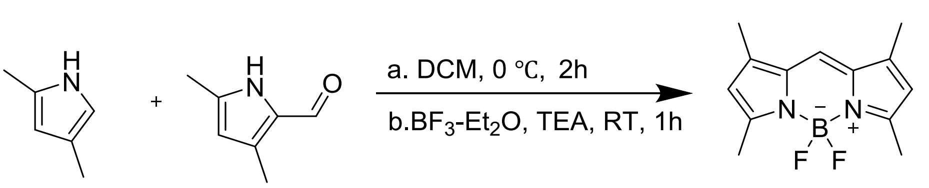

3,5-dimethyl BODIPY

A solution of 2,4-dimethyl-1-pyrrole (2 g, 21.02 mmol) and 3,5-dimethyl-1H-pyrrole-2-carbaldehyde (2.59 g, 21.02 mmol) in DCM (100 mL) and cooled to 0°C. After $POCl_3$

(1.96 mL, 21.02 mmol) was added slowly, the mixture was stirred at room temperature for 2 h. $BF_3 \cdot Et_2O$ (15.57 mL, 126.12 mmol) and Et_3N (16.75 mL, 126.12 mmol) were added sequentially, and the resulting mixture was stirred at room temperature for 1 h. The solution was washed with H_2O and dried with Na_2SO_4. The solvent was removed, and the residue was purified by silica gel column chromatography (petroleum ether/ethyl acetate = 40:1 ~ 20: 1) to give 3,5-dimethyl BODIPY (1.13 g, yield 21.67%). ^1H NMR (400 MHz, DMSO-d_6) δ = 7.68 (s, 1H), 6.21 (s, 2H), 2.42 (s, 6H), 2.27 (s, 6H).

4.2 Synthesis of compound of 3,8-dimethyl BODIPY

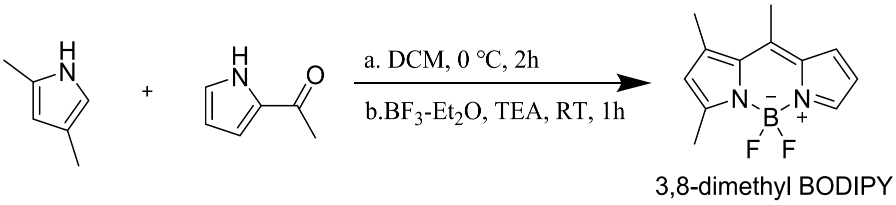

A solution of 2,4-dimethyl-1-pyrrole (2 g, 21.02 mmol) and 2-acetylpyrrole (2.29 g, 21.02 mmol) in dichloromethane (DCM, 100 mL) was cooled to 0°C. $POCl_3$ (1.96 mL, 21.02 mmol) was added slowly, and the mixture was stirred at room temperature for 2 hours. $BF_3 \cdot Et_2O$ (15.57 mL, 126.12 mmol) and Et_3N (16.75 mL, 126.12 mmol) were added sequentially, and the resulting mixture was stirred at room temperature for 1 hour. The solution was washed with H_2O and dried over Na_2SO_4. The solvent was removed, and the residue was purified by silica gel column chromatography (petroleum ether/ethyl acetate = 40:1~ 20:1) to give 3,8-dimethyl BODIPY (1.38 g, yield 28.05%). ^1H NMR (400 MHz, DMSO-d_6) δ = 7.64 (s, 1H), 7.42 (s, 1H), 6.49 (s, 1H), 6.39 (s, 1H), 2.64 (s, 3H), 2.48 (s, 3H), 2.44 (s, 3H).

4.3 General procedure for the synthesis of 3-HS-X-BOD

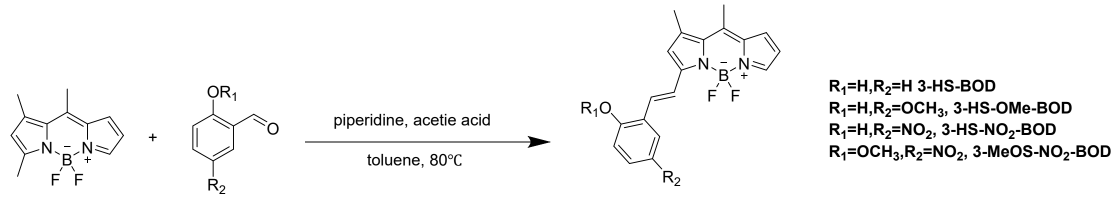

To a solution of 3,8-dimethyl BODIPY (1 eq) and corresponding aldehydes (1 eq) in toluene (10 mL) was added a catalytic amount of piperidine and acetic acid. The reaction mixture was heated to 80°C and stirred for 30 minutes. The solution was washed with H_2O (50 mL * 3) and extracted with ethyl acetate (100 mL * 3). The combined organic layers were dried over Na_2SO_4 and filtered. The solvent was removed, and the residue was purified by silica gel chromatography (petroleum ether: ethyl acetate = 5: 1) to afford **3-HS-X-BOD**.

Compound **3-HS-BOD** was obtained as a red solid (75 mg, yield 34.61%). ^{1}H NMR (400 MHz, DMSO-d_6) δ 10.28 (s, 1H), 7.71 (dd, *J* = 8.0, 5.0, 3.3 Hz, 3H), 7.51 (d, *J* = 16.1 Hz, 1H), 7.27 – 7.22 (m, 1H), 7.12 (d, *J* = 3.9 Hz, 1H), 6.94 (d, *J* = 8.1 Hz, 1H), 6.89 (t, *J* = 7.5 Hz, 1H), 6.53 (dd, J = 4.0, 2.1 Hz, 1H), 6.41 (s, 1H), 2.50 (s, 3H), 2.42 (s, 3H). ^{13}C NMR (100 MHz, DMSO-d_6) δ 159.56, 156.94, 145.51, 142.71, 138.20, 132.63, 132.24, 131.55, 128.88, 126.38, 123.22, 122.89, 121.88, 120.03, 116.66, 116.41, 16.97, 15.06. HRMS: calculated. for $C_{19}H_{18}BF_2N_2O$ [M+H] $^+$: 339.1474, found 339.1475.

Compound **3-HS-OMe-BOD** was obtained as a red solid (109 mg, yield 46.19%). ^{1}H NMR (400 MHz, DMSO-d_6) δ 9.80 (s, 1H), 7.74 – 7.67 (m, 2H), 7.47 (d, *J* = 16.0 Hz, 1H), 7.26 (d, *J* = 2.3 Hz, 1H), 7.11 (d, *J* = 4.0 Hz, 1H), 6.85 (d, *J* = 2.1 Hz, 2H), 6.51 (dd, *J* = 4.0, 2.1 Hz, 1H), 6.39 (s, 1H), 3.72 (s, 3H), 2.48 (s, 3H), 2.40 (s, 3H). ^{13}C NMR (100 MHz, DMSO-d_6) δ 159.57, 152.89, 151.13, 145.53, 142.61, 138.20, 138.05, 132.64, 132.23, 126.37, 123.24, 123.14, 122.14, 118.07, 117.52, 116.40, 112.60, 56.00, 16.91, 15.06. HRMS: calculated. for $C_{20}H_{20}BF_2N_2O_2$ [M+H]$^+$: 369.1580, found 369.1581.

Compound **3-HS-NO$_2$-BOD** was obtained as a red solid (60 mg, yield 24.43%).^{1}H NMR (400 MHz, DMSO-d_6) δ 8.59 (d, *J* = 2.9 Hz, 1H), 8.14 (dd, *J* = 9.1, 2.8 Hz, 1H), 7.88 (d, *J* = 16.1 Hz, 1H), 7.72 (s, 1H), 7.41 (d, *J* = 16.1 Hz, 1H), 7.17 – 7.07 (m, 2H), 6.52 (q, J = 3.3 Hz, 1H), 6. 41 (s, 1H), 2.50 (s, 3H), 2.40 (s, 3H). ^{13}C NMR (100 MHz, DMSO-d_6) δ 162.58, 160.55, 146.01, 141.67, 140.52, 138.78, 135.56, 132.77, 132.29, 130.10, 126.85, 126.66, 125.19, 124.88, 123.47, 117.00, 116.66,16.79, 15.12. HRMS: calculated. for $C_{19}H_{17}BF_2N_3O_3$ $[M+H]^+$: 384.1325, found 384.1324.

Compound **3-MeOS-NO$_2$-BOD** was obtained as a red solid (68 mg, yield 27.71%).^{1}H NMR (400 MHz, DMSO-d_6) δ 8.66 (d, J = 2.8 Hz, 1H), 8.30 (dd, J = 9.2, 2.7 Hz, 1H), 7.89 (d, J = 16.2 Hz, 1H), 7.75 (s, 1H), 7.44 – 7.32 (m, 2H), 7.16 (d, J = 4.0 Hz, 1H), 6.54 (dd, J = 4.1, 2.1 Hz, 1H), 6.44 (s, 1H), 4.02 (s, 3H), 2.52 (s, 3H), 2.40 (s, 3H). ^{13}C NMR (100 MHz, DMSO-d_6) δ 162.74, 160.82, 146.18, 141.54, 141.32, 138.97, 134.57, 132.81, 132.31, 126.91, 126.80, 125.78, 125.18, 124.40, 123.51, 116.72, 112.86, 57.42, 16.70, 15.15. HRMS: calculated. for $C_{20}H_{19}BF_2N_3O_3$ $[M+H]^+$: 398.1482, found 398.1480.

4.4 General procedure for the synthesis of 3,5-HS-X-BOD

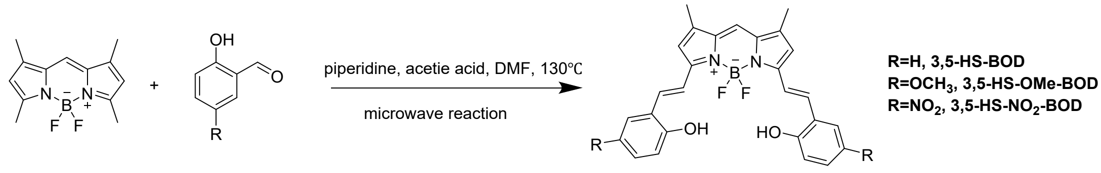

3,5-HS-X-BOD

To a solution of 3,8-dimethyl BODIPY (1 eq) and corresponding aldehydes (10 eq) in DMF (10 mL) was added with a catalytic amount of piperidine and acetic acid. The reaction mixture was placed in a microwave reactor and then was heated to 130°C and stirred for 10~30 min. The solution was washed with H_2O (50 mL * 3) and extracted with ethyl acetate (100 mL * 3). The combined organic layers were dried over Na_2SO_4 and filtered. The solvent was removed, and the residue was purified by silica gel chromatography (petroleum ether: ethyl acetate =3: 1 ~ 1: 1) to afford **3,5-HS-X-BOD**.

Compound **3,5-HS-BOD** was obtained as a purple solid (85 mg, yield 23.11%). ^{1}H NMR (400 MHz, DMSO-d_6) δ 10.22 (s, 2H), 7.66 (d, J = 16.4 Hz, 2H), 7.62 – 7.55 (m, 3H), 7.50 (d, J = 7.7 Hz, 2H), 7.20 (t, J = 7.7 Hz, 2H), 6.97 (s, 2H), 6.90 (t, J = 8.5 Hz, 4H), 2.34 (s, 6H). ^{13}C NMR (100 MHz, DMSO-d_6) δ 156.54, 154.13, 141.19, 135.49, 132.88, 130.90, 130.11, 128.07, 123.56, 120.09, 118.87, 116.67, 116.14, 11.55. HRMS: calculated. for $C_{27}H_{24}BF_2N_2O_2$ $[M+H]^+$: 457.1893, found 457.1892.

Compound **3,5-HS-OMe-BOD** was obtained as a dark brown solid (66 mg, yield 21.14%). ^{1}H NMR (400 MHz, DMSO-*d*$_6$) δ 9.80 (s, 2H), 7.60 (s, 4H), 7.56 (s, 1H), 6.97 (d, *J* = 13.8 Hz, 4H), 6.84 (s, 4H), 3.73 (s, 6H), 2.33 (s, 6H). ^{13}C NMR (100 MHz, DMSO-*d*$_6$) δ 154.39, 153.10, 151.15, 141.40, 135.85, 133.37, 130.36, 124.23, 119.73, 119.08, 117.74, 117.20, 116.46, 113.00, 56.25, 11.78. HRMS: calculated. for $C_{29}H_{28}BF_2N_2O_4$ $[M+H]^+$: 517.2105, found 517.2101.

Compound **3,5-HS-NO$_2$-BOD** was obtained as a brown solid (78 mg, yield 23.61%) ^{1}H NMR (400 MHz, DMSO-*d*$_6$) δ 8.34 (d, *J* = 2.8 Hz, 2H), 8.10 (dd, *J* = 9.0, 2.8 Hz, 2H), 7.77 (d, *J* = 16.4 Hz, 2H), 7.66 (d, *J* = 17.6 Hz, 3H), 7.10 - 7.01 (m, 4H), 2.34 (s, 6H). ^{13}C NMR (100 MHz, DMSO-*d*$_6$) δ 162.71, 153.87, 141.70, 140.33, 135.94, 131.63, 130.09, 126.13, 124.67, 124.08, 121.48, 120.00, 117.08, 116.72, 11.59. HRMS: calculated. for $C_{27}H_{22}BF_2N_4O_6$ $[M+H]^+$: 547.1595, found 547.1592.

4.5 General procedure for the synthesis of 3,8-HS-X-BOD

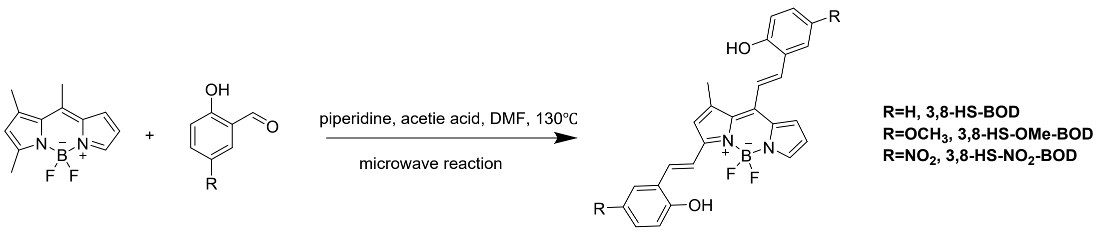

3,8-HS-X-BOD

To a solution of 3,8-dimethyl BODIPY (1 eq) and corresponding aldehydes (10 eq) in DMF (10 mL) was added with a catalytic amount of piperidine and acetic acid. The reaction mixture was placed in a microwave reactor and then was heated to 130°C and stirred for 10~30 min. The solution was washed with H_2O (50 mL * 3) and extracted with ethyl acetate (100 mL * 3). The combined organic layers were dried over Na_2SO_4

and filtered. The solvent was removed, and the residue was purified by silica gel chromatography (petroleum ether: ethyl acetate =5: 1 ~ 2: 1) to afford **3,8-HS-X-BOD**.

Compound **3,8-HS-BOD** was obtained as a dark green solid (95 mg, yield 33.52%). ^{1}H NMR (400 MHz, DMSO-*d₆*) δ 10.33 (s, 2H), 7.81 – 7.69 (m, 5H), 7.60 – 7.47 (m, 2H), 7.25 (q, *J* = 6.9 Hz, 2H), 7.18 (s, 1H), 7.11 (d, *J* = 3.9 Hz, 1H), 6.92 (dt, *J* = 15.3, 7.6 Hz, 4H), 6.59 – 6.50 (m, 1H), 2.49 (s, 3H). ^{13}C NMR (100 MHz, DMSO-d_6) δ 157.18, 157.10, 156.91, 144.86, 140.53, 137.71, 137.19, 136.10, 134.30, 132.36, 131.60, 131.46, 128.89, 128.79, 125.30, 123.18, 123.11, 122.25, 120.15, 120.07, 119.67, 118.73, 116.81, 116.68, 116.20, 40.64, 40.43, 40.22, 40.02, 39.81, 39.60, 39.39, 17.21. HRMS: calculated. for $C_{26}H_{22}BF_2N_2O_2$ [M+H]$^+$: 443.1736, found 443.1733.

Compound **3,8-HS-OMe-BOD** was obtained as a dark green solid (105 mg, yield 32.62%). ^{1}H NMR (400 MHz, DMSO-d_6) δ 9.94 (s, 1H), 9.83 (s, 1H), 7.80 – 7.73 (m, 3H), 7.71 (t, *J* = 1.6 Hz, 1H), 7.52 (d, *J* = 16.1 Hz, 1H), 7.29 (t, *J* = 1.6 Hz, 1H), 7.17 (s, 1H), 7.11 (d, *J* = 4.0 Hz, 1H), 7.00 (d, *J* = 2.5 Hz, 1H), 6.87 (d, *J* = 2.4 Hz, 4H), 6.56 – 6.54 (m, 1H), 3.74 (d, *J* = 4.9 Hz, 6H), 2.49 (s, 3H). ^{13}C NMR (100 MHz, DMSO-d_6) δ 157.05, 152.93, 152.80, 151.41, 151.10, 144.84, 140.45, 137.57, 137.28, 136.11, 134.35, 132.35, 130.11, 125.34, 123.36, 122.52, 119.71, 119.01, 118.23, 118.02, 117.70, 117.54, 116.24, 112.50, 112.46, 56.03, 55.93, 17.15. HRMS: calculated. for $C_{28}H_{26}BF_2N_2O_4$ [M+H]$^+$: 503.1948, found 503.1948.

Compound **3,8-HS-NO$_2$-BOD** was obtained as a black solid (120 mg, yield 35.18%). ^{1}H NMR (400 MHz, DMSO-d_6) δ 8.60 (s, 1H), 8.37 (s, 1H), 8.13 (t, *J* = 9.4 Hz, 2H), 7.94 (t, *J* = 15.2 Hz, 2H), 7.82 – 7.74 (m, 2H), 7.45 (d, *J* = 16.1 Hz, 1H), 7.20 (d, *J* = 5.6 Hz, 2H), 7.09 (t, *J* = 9.9 Hz, 2H), 6.58 (d, *J* = 4.1 Hz, 1H), 2.47 (s, 3H). ^{13}C NMR (100 MHz, DMSO-d_6) δ 162.96, 162.74, 156.50, 144.98, 140.68, 140.47, 140.37, 138.95, 135.70, 134.29, 132.69, 130.10, 126.83, 126.67, 126.58, 125.39, 125.29, 125.21, 123.67, 123.59, 121.40, 119.80, 117.23, 117.06, 116.96, 17.04. HRMS: calculated. for $C_{26}H_{20}BF_2N_2O_6$ [M+H]$^+$: 533.1438, found 533.1432.

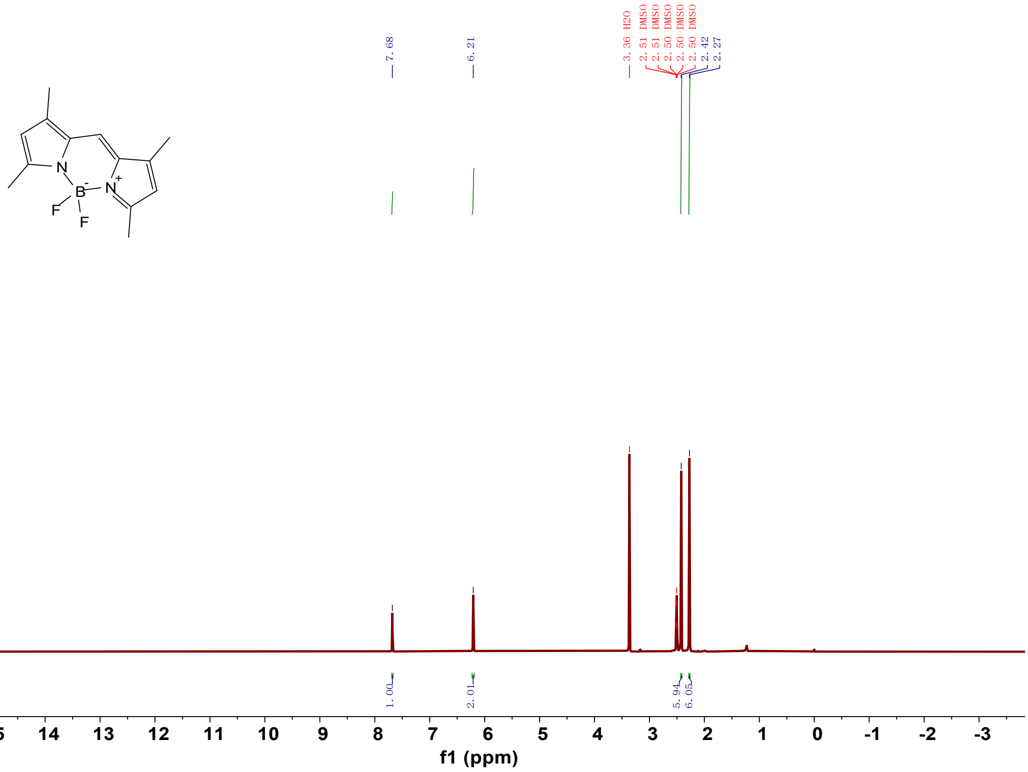

Figure S18. ^{1}**H NMR** spectrum of 3,5-dimethyl BODIPY.

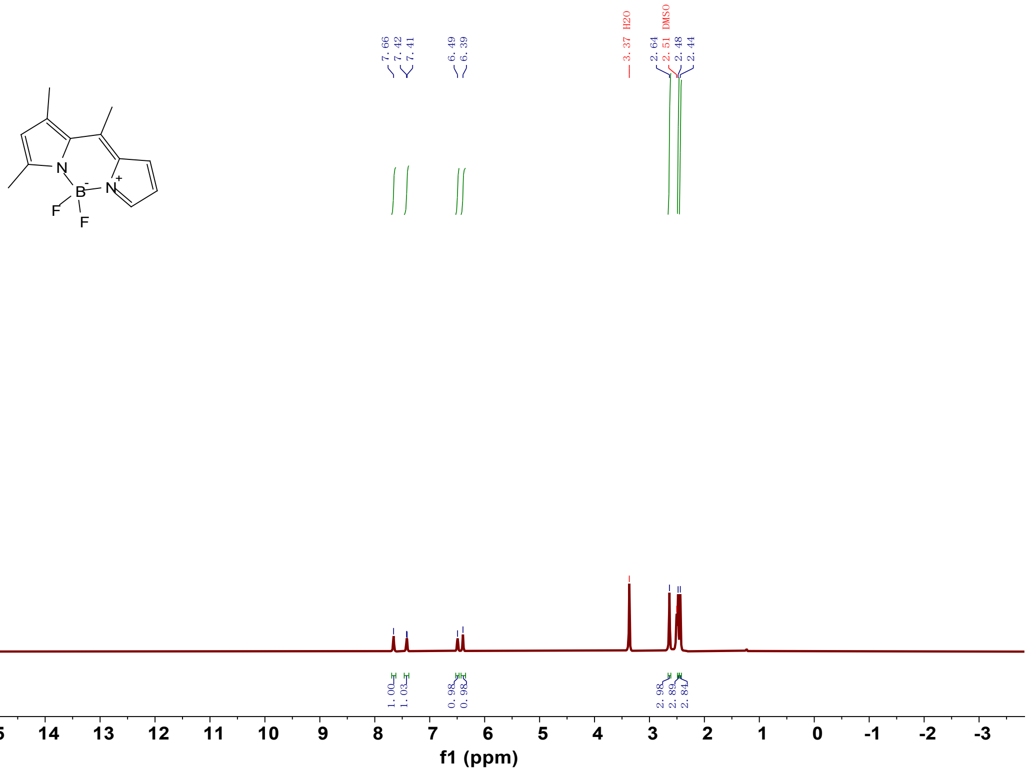

Figure S19. ^{1}**H NMR** spectrum of 3,8-dimethyl BODIPY.

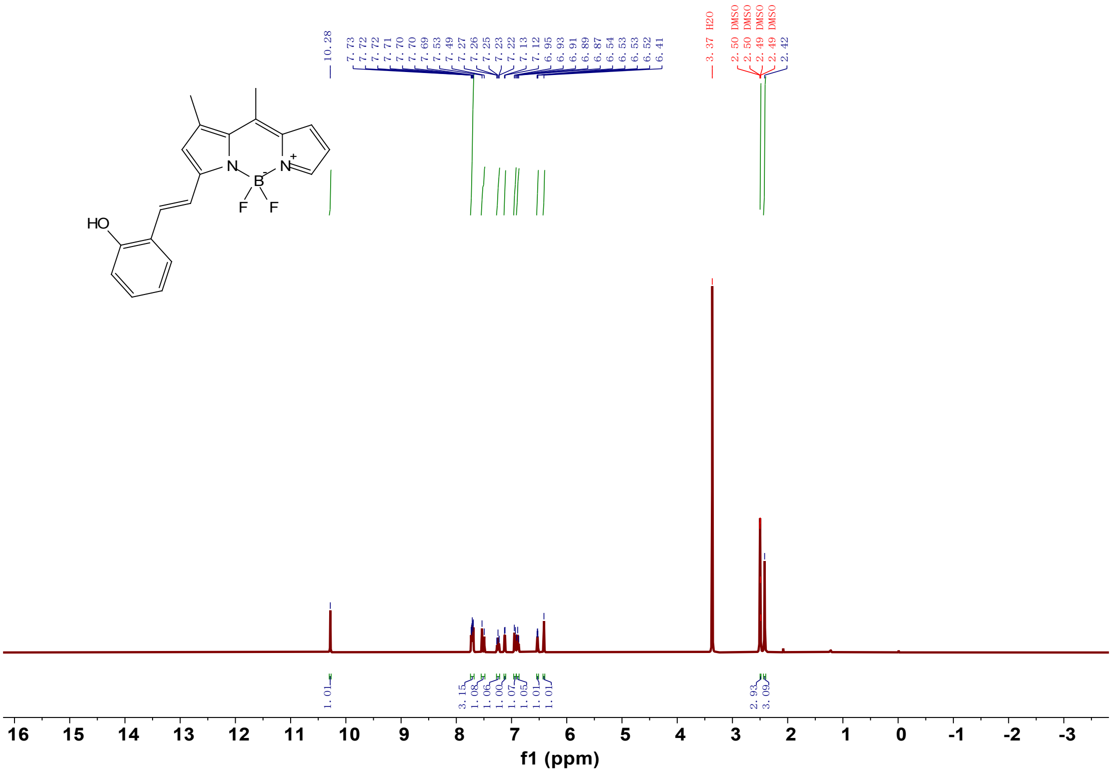

Figure S20. **^{1}H NMR** spectrum of 3-HS-BOD.

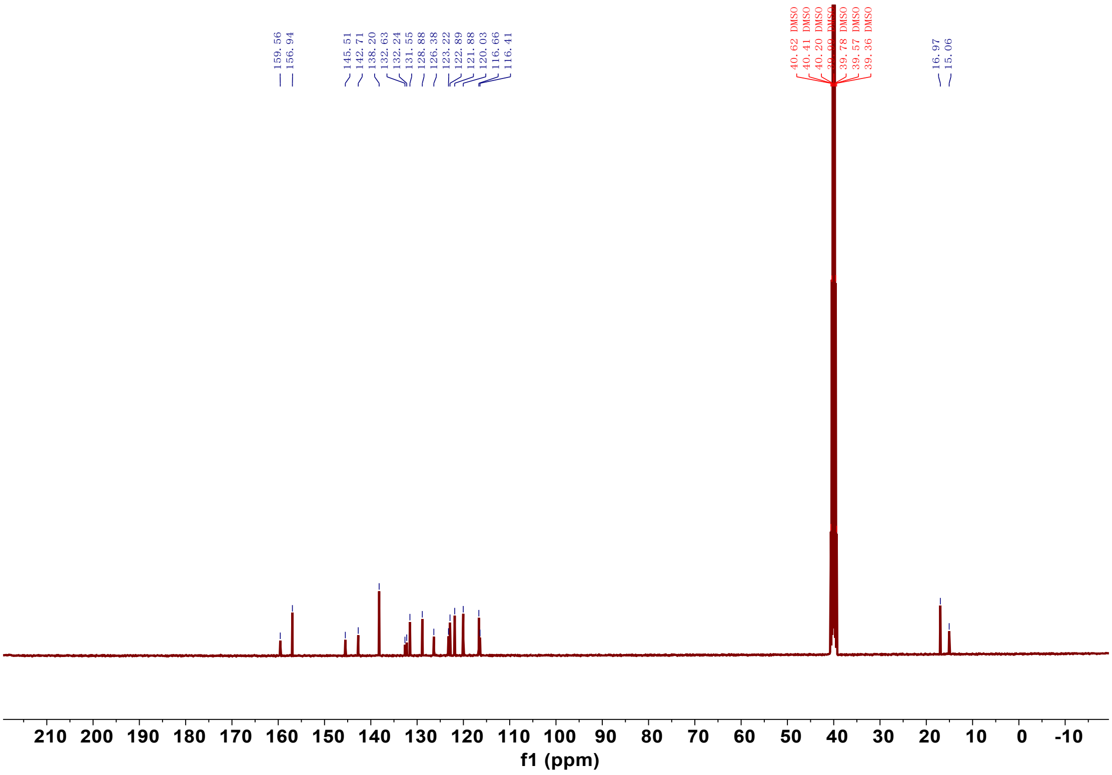

Figure S21. **^{13}C NMR** spectrum of 3-HS-BOD.

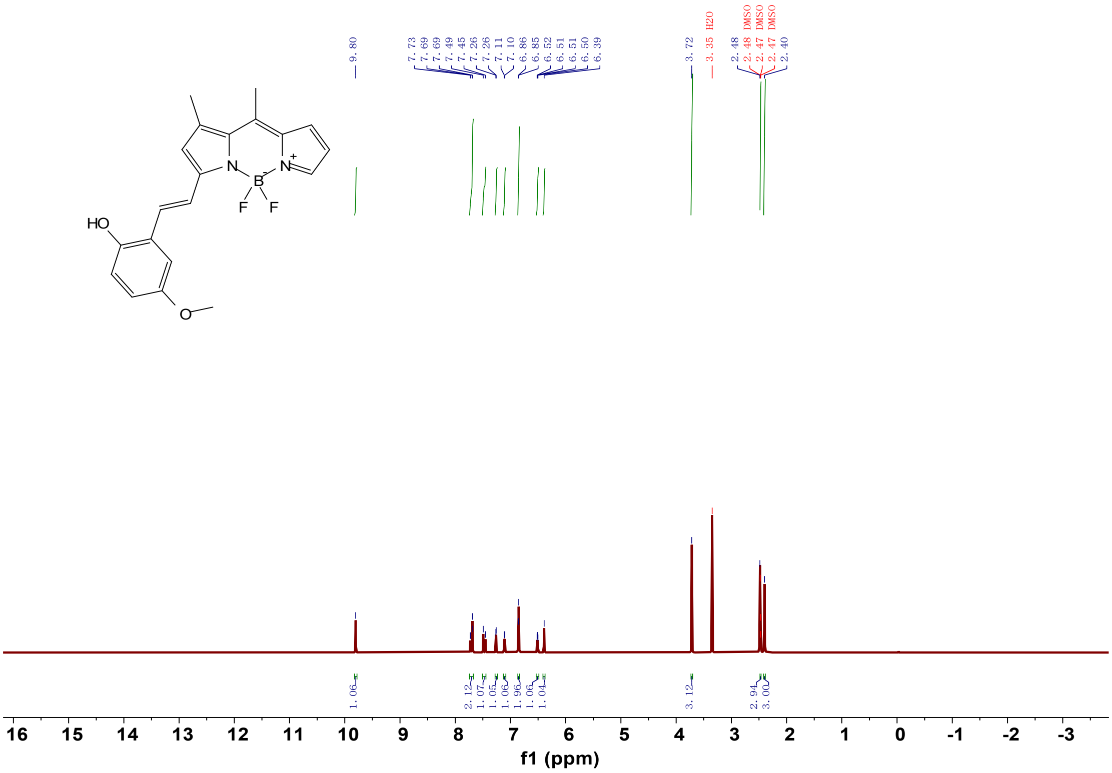

Figure S22. **^{1}H NMR** spectrum of 3-HS-OMe-BOD.

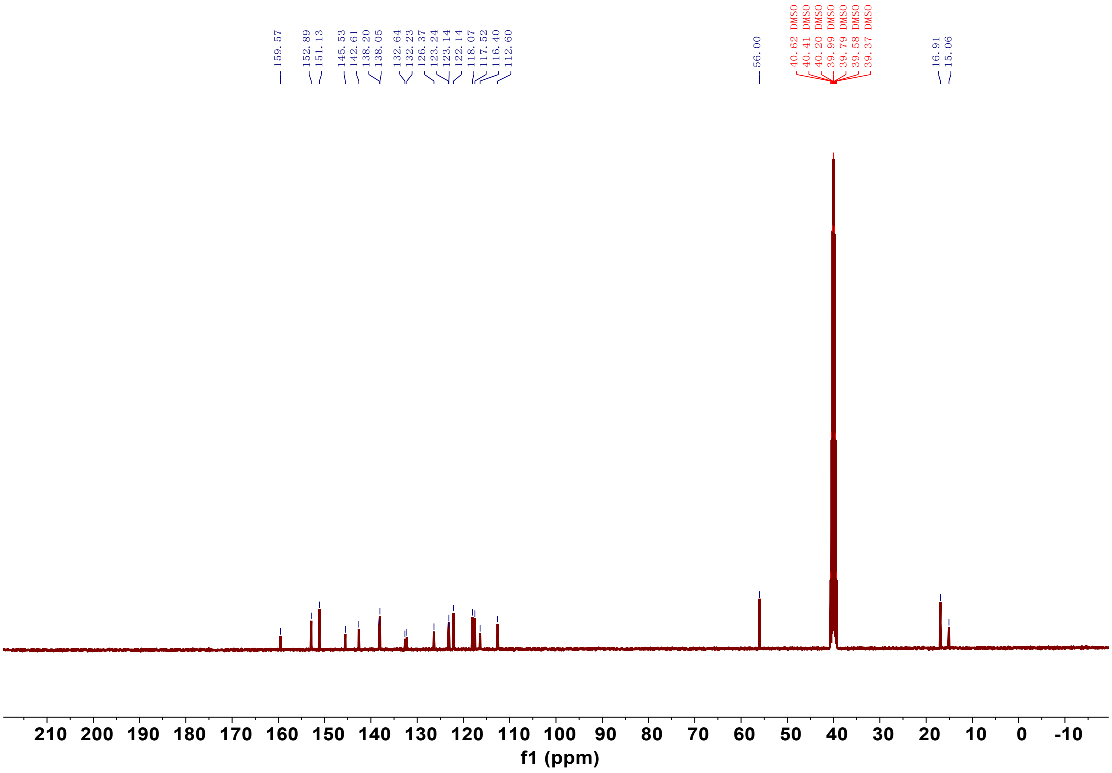

Figure S23. **^{13}C NMR** spectrum of 3-HS-OMe-BOD.

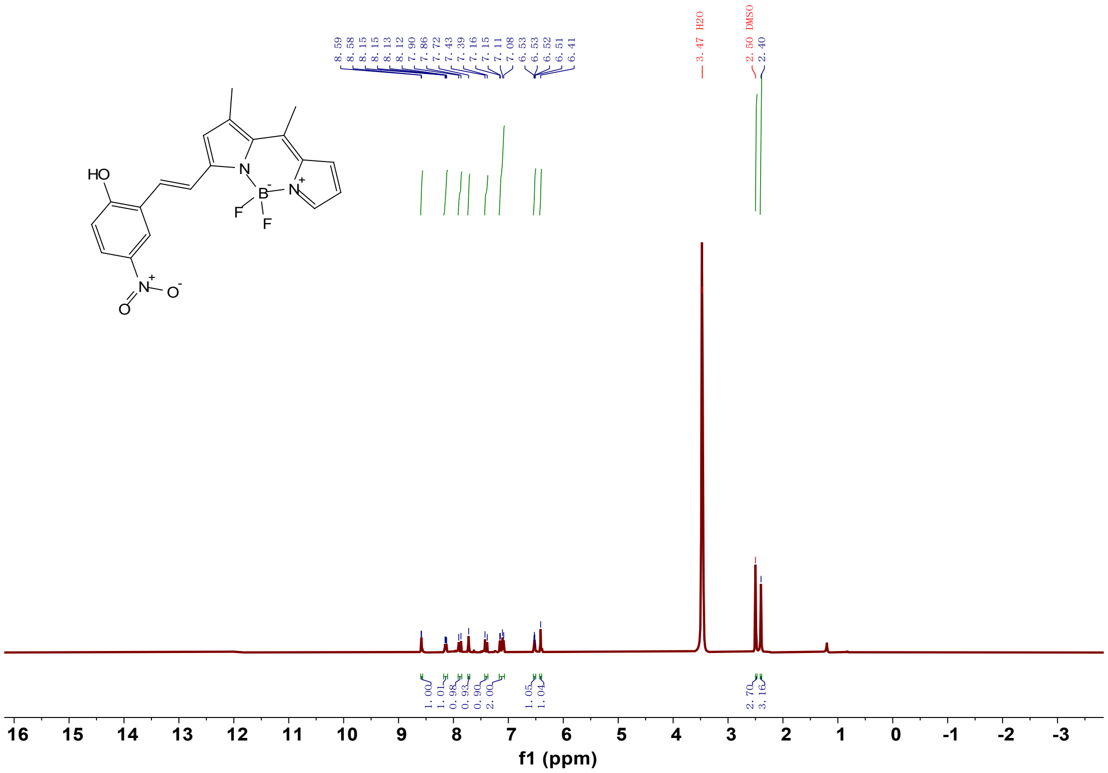

Figure S24. **^{1}H NMR** spectrum of 3-HS-NO$_2$-BOD.

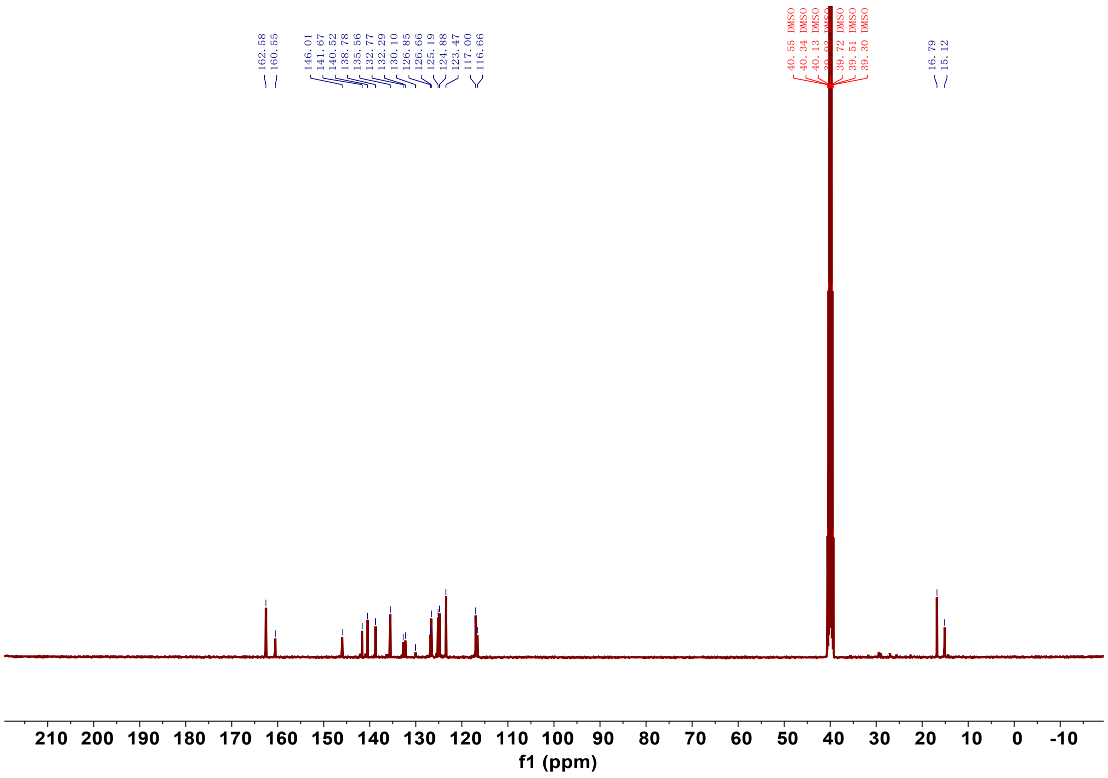

Figure S25. **^{13}C NMR** spectrum of 3-HS-NO$_2$-BOD.

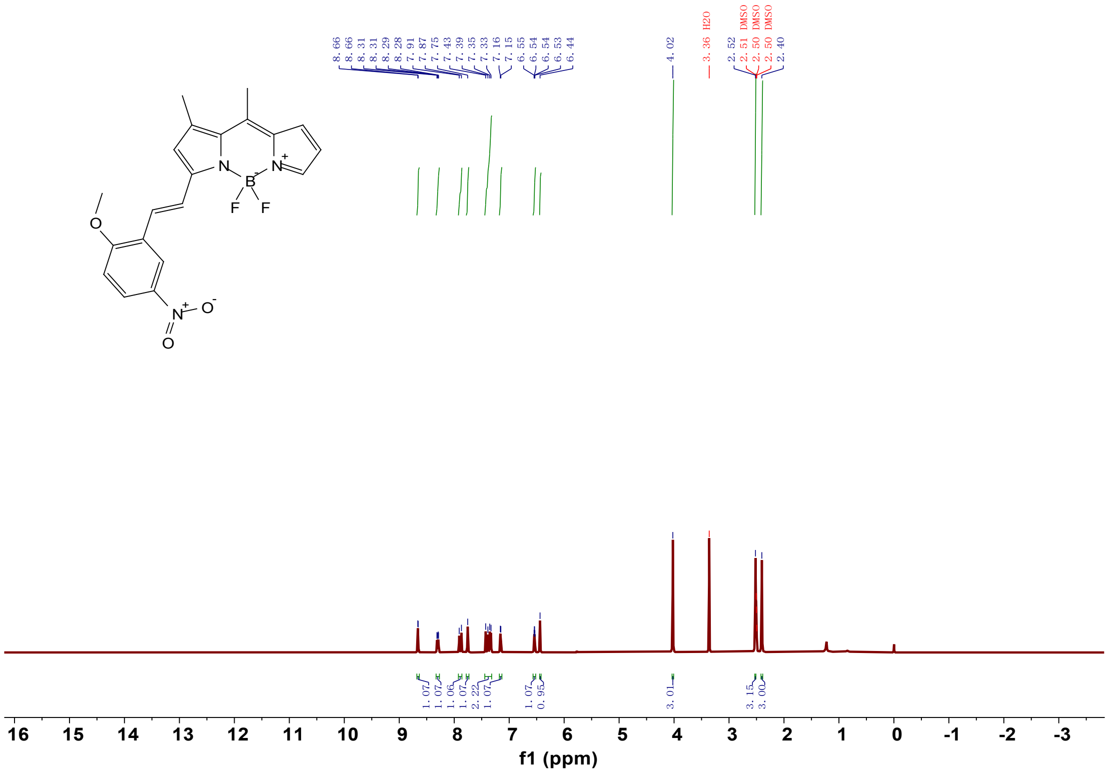

Figure S26. ^{1}**H NMR** spectrum of 3-MeOS-NO_2-BOD.

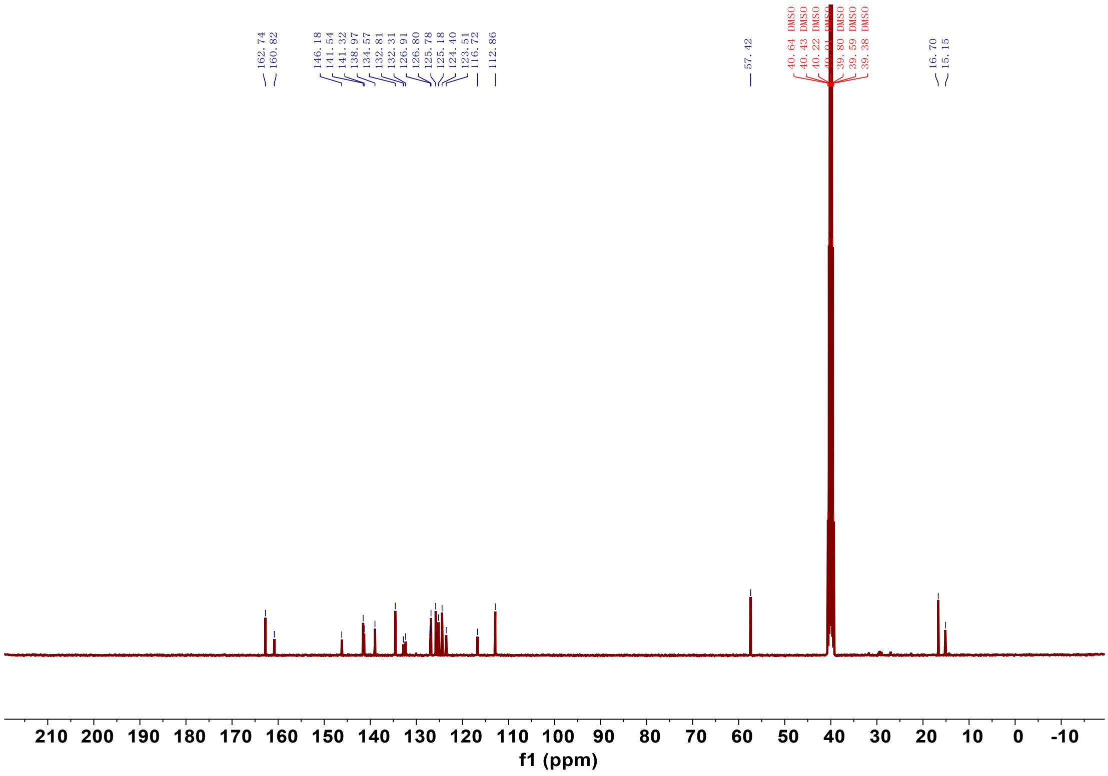

Figure S27. ^{13}**C NMR** spectrum of 3-MeOS-NO_2-BOD.

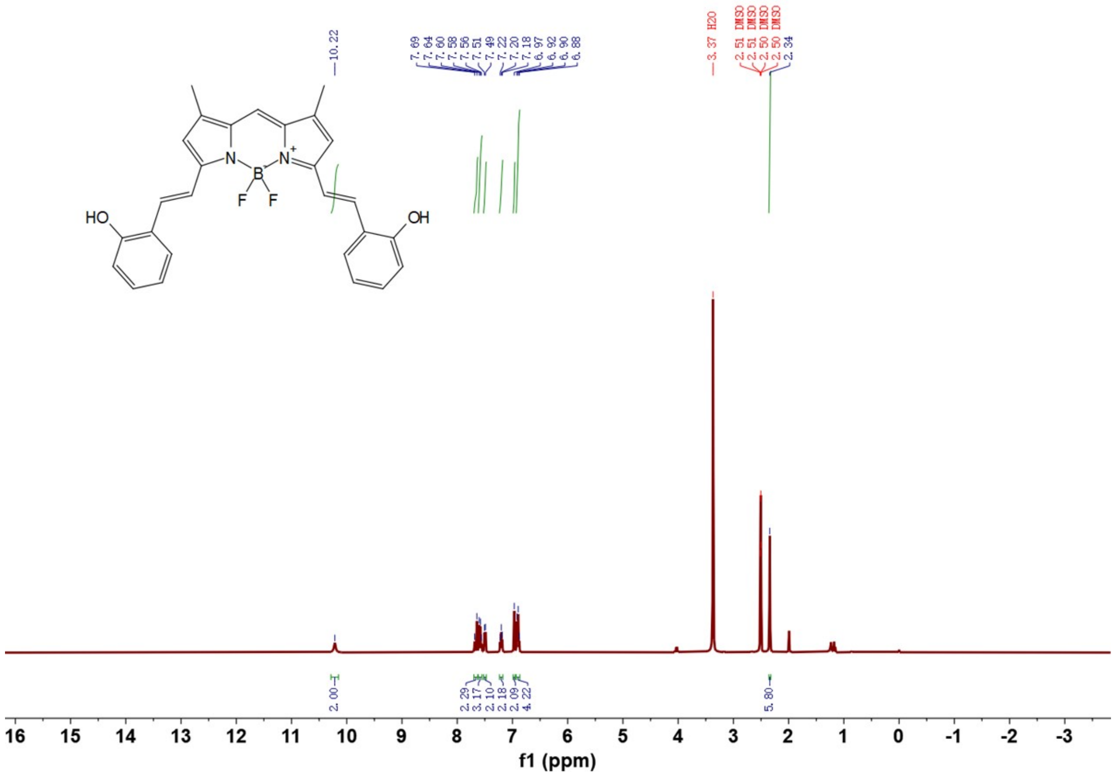

Figure S28. ^{1}**H NMR** spectrum of 3,5-HS-BOD.

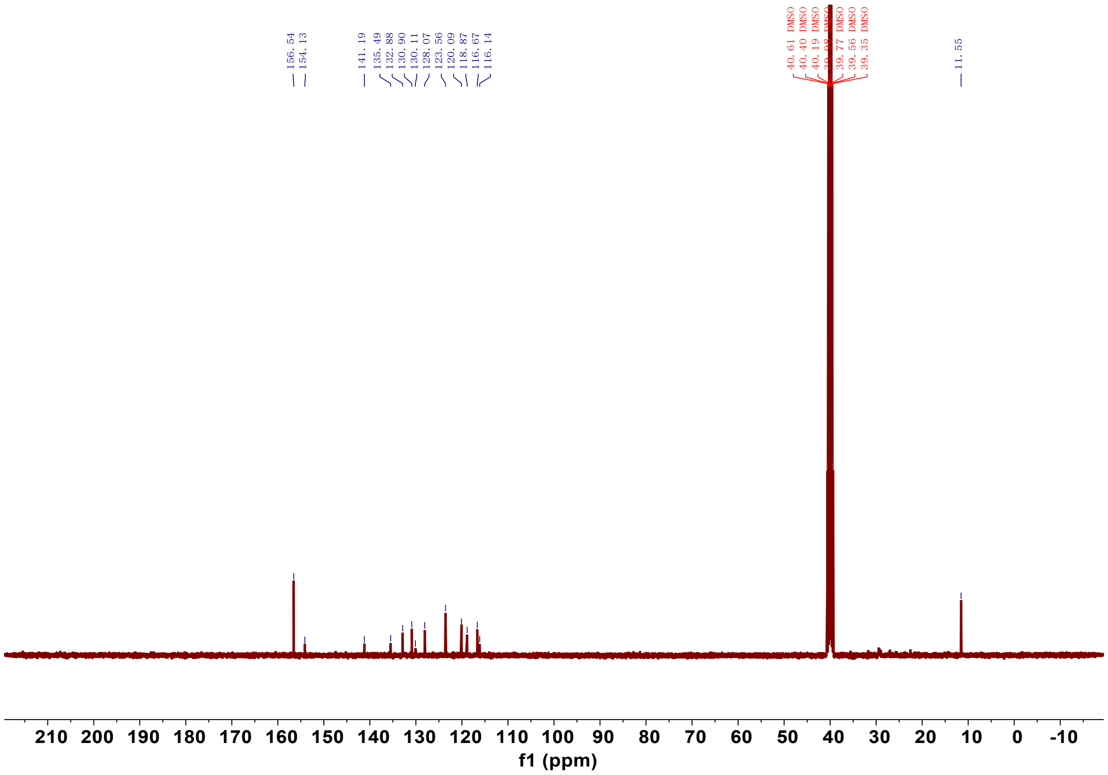

Figure S29. ^{13}**C NMR** spectrum of 3,5-HS-BOD.

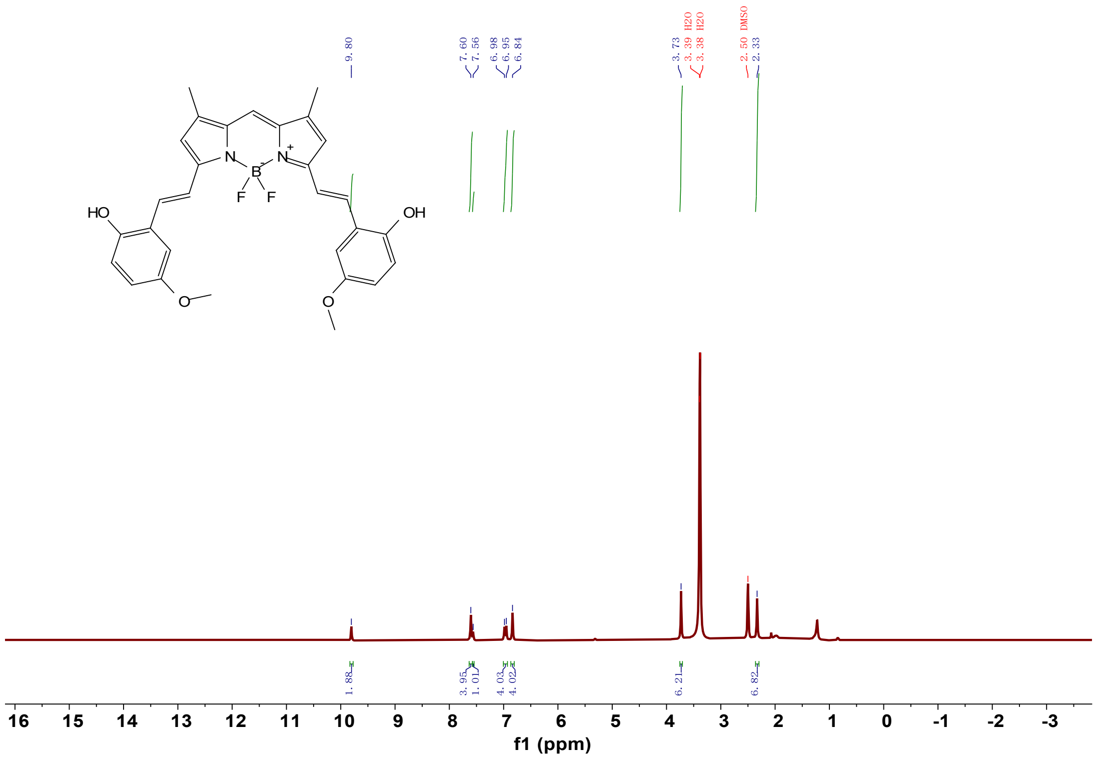

Figure S30. ^{1}**H NMR** spectrum of 3,5-HS-OMe-BOD.

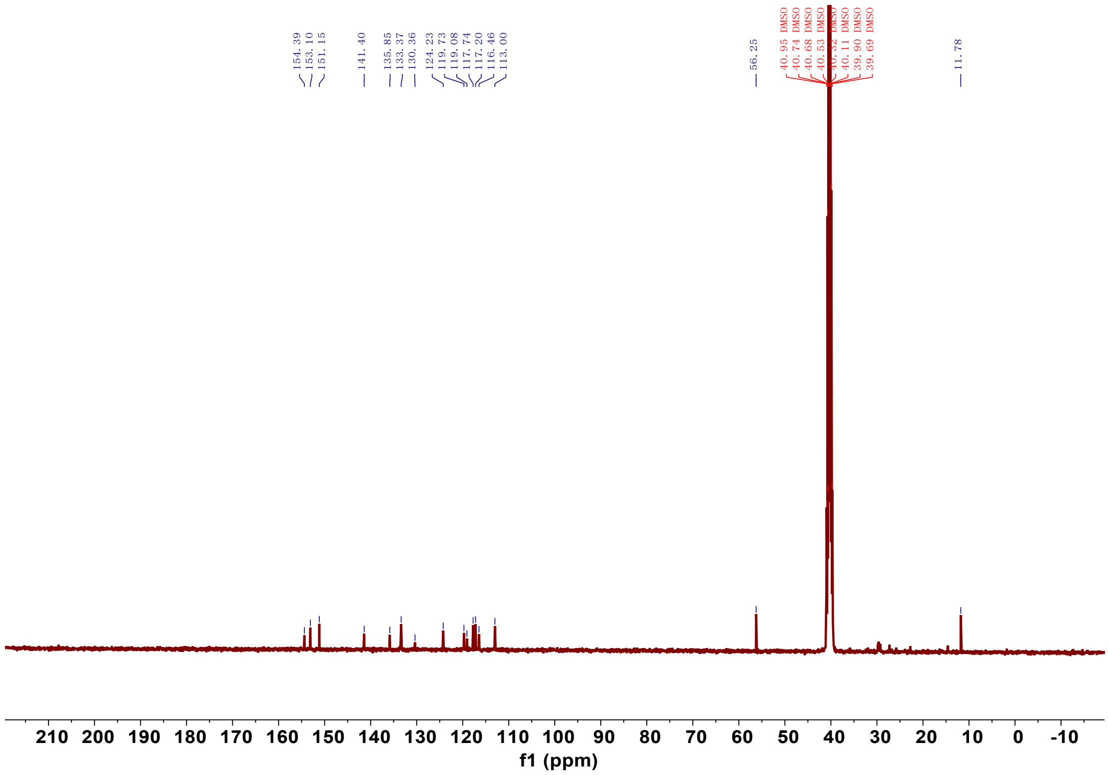

Figure S31. ^{13}**C NMR** spectrum of 3,5-HS-OMe-BOD.

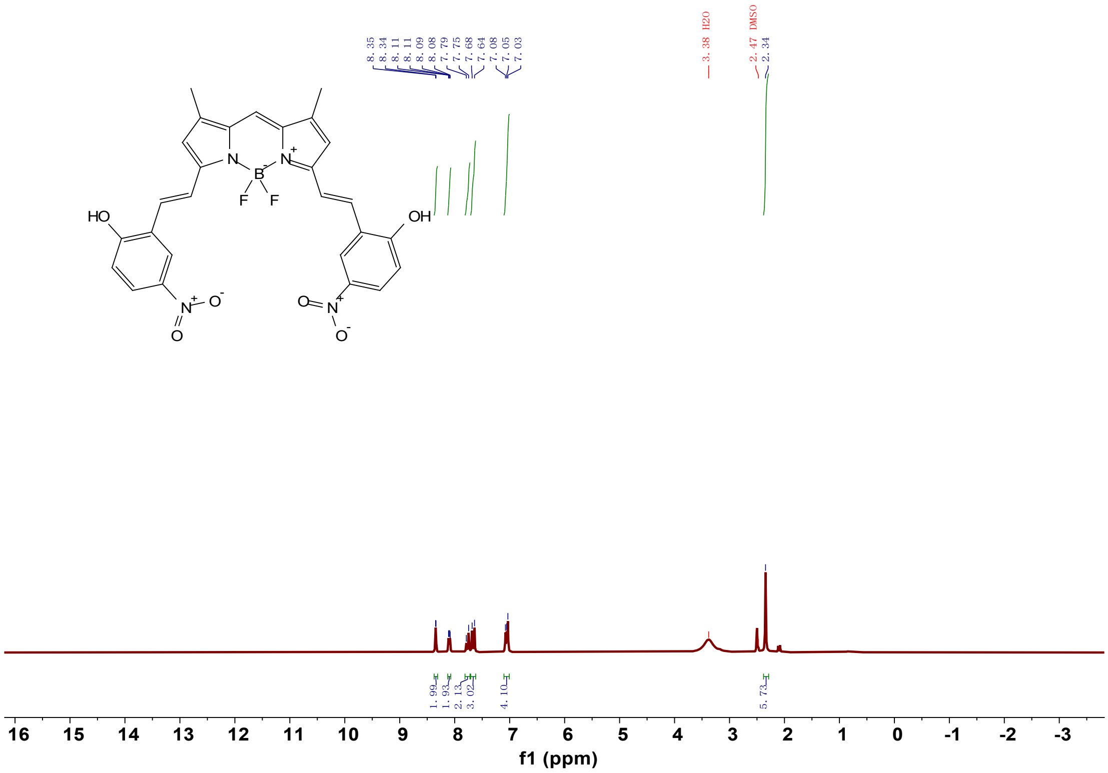

Figure S32. ^{1}**H NMR** spectrum of 3,5-HS-NO_2-BOD.

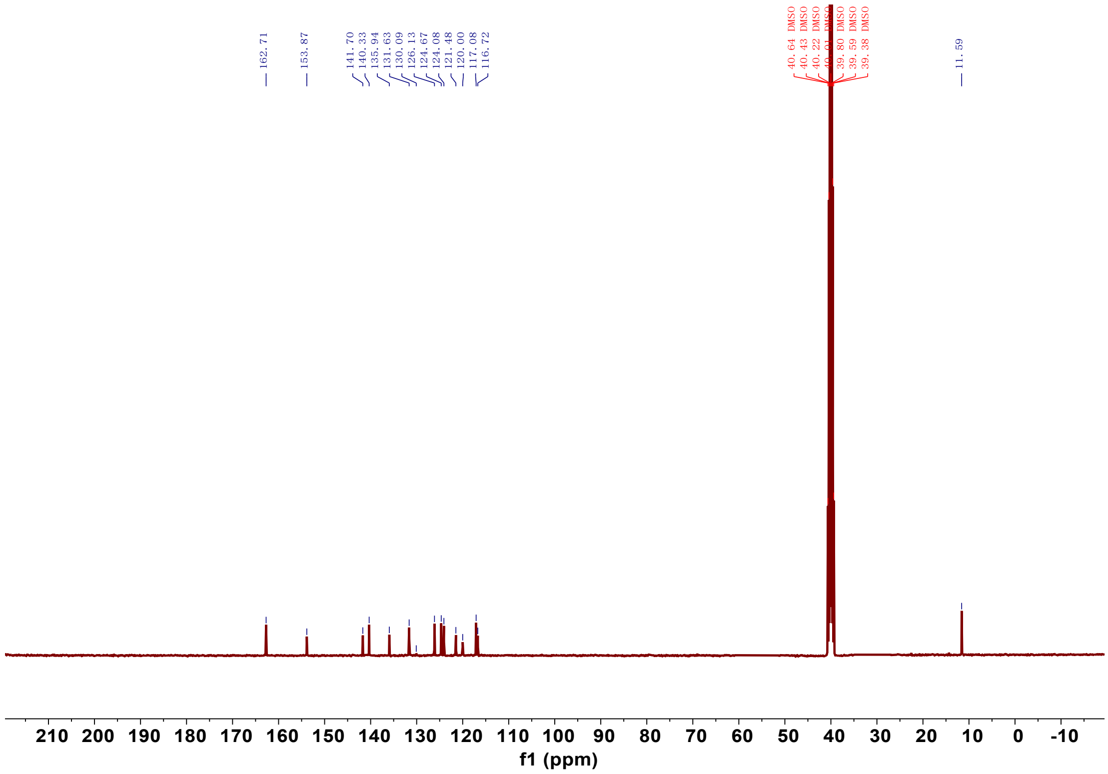

Figure S33. ^{13}**C NMR** spectrum of 3,5-HS-NO_2-BOD.

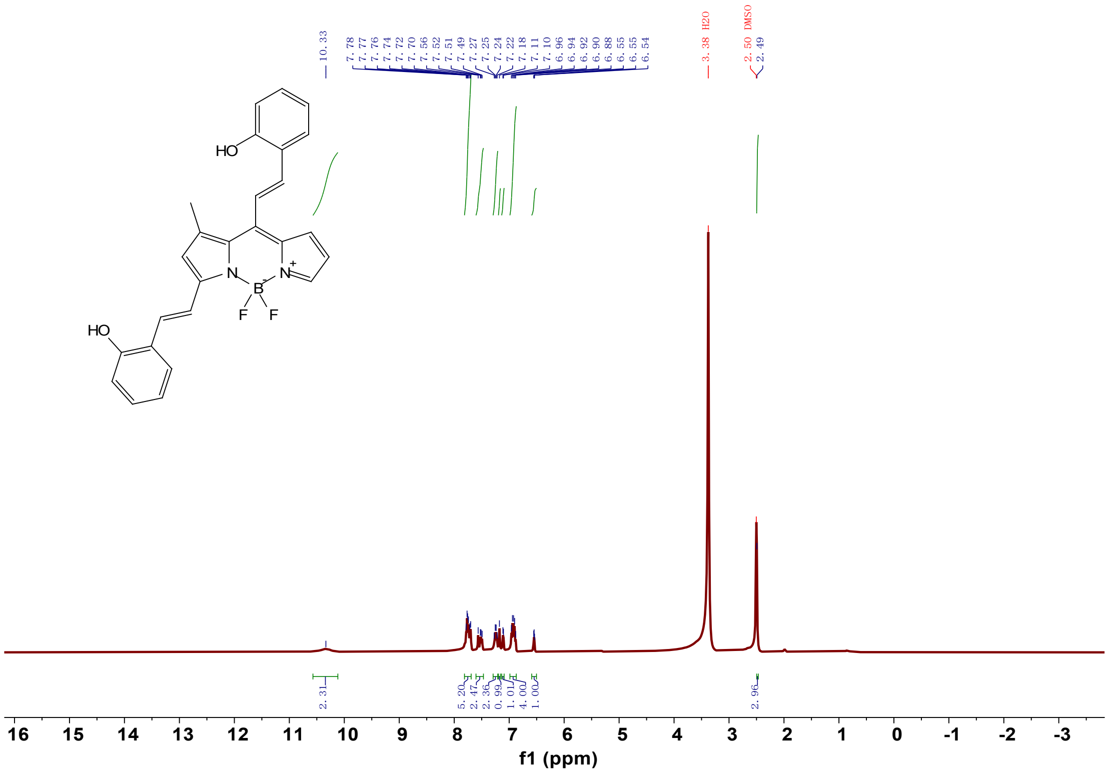

Figure S34. ^{1}H NMR spectrum of 3,8-HS-BOD.

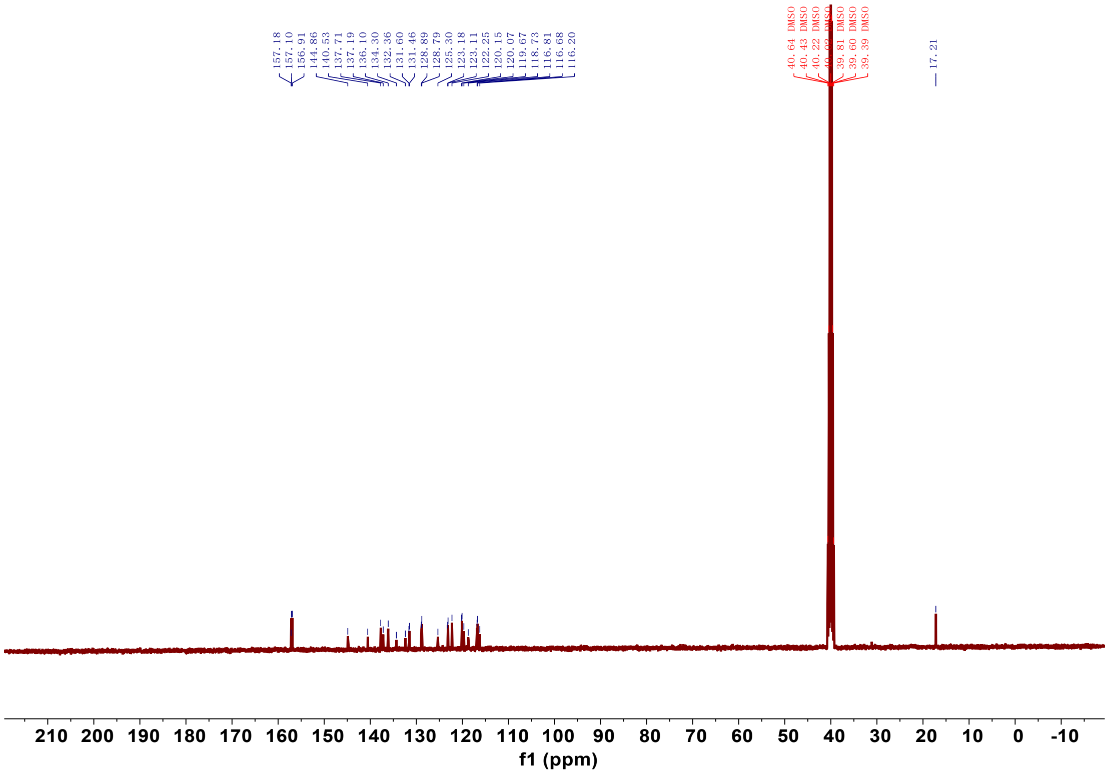

Figure S35. ^{13}C NMR spectrum of 3,8-HS-BOD.

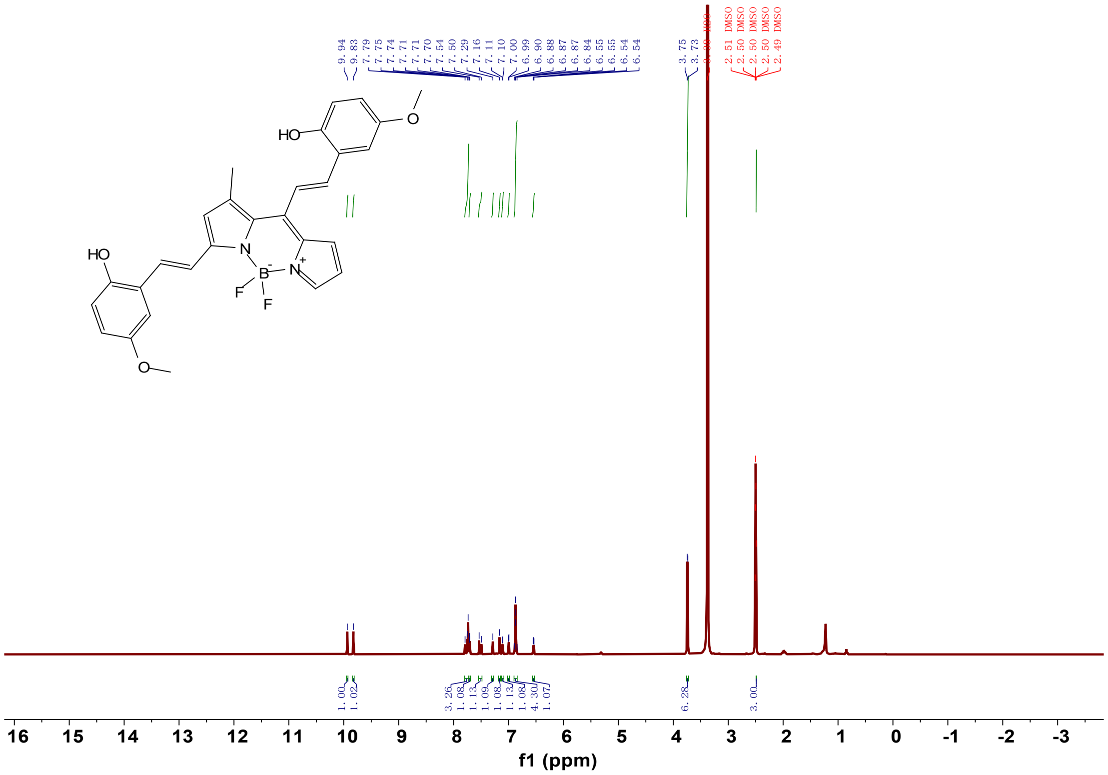

Figure S36. ^{1}H NMR spectrum of 3,8-HS-OMe-BOD.

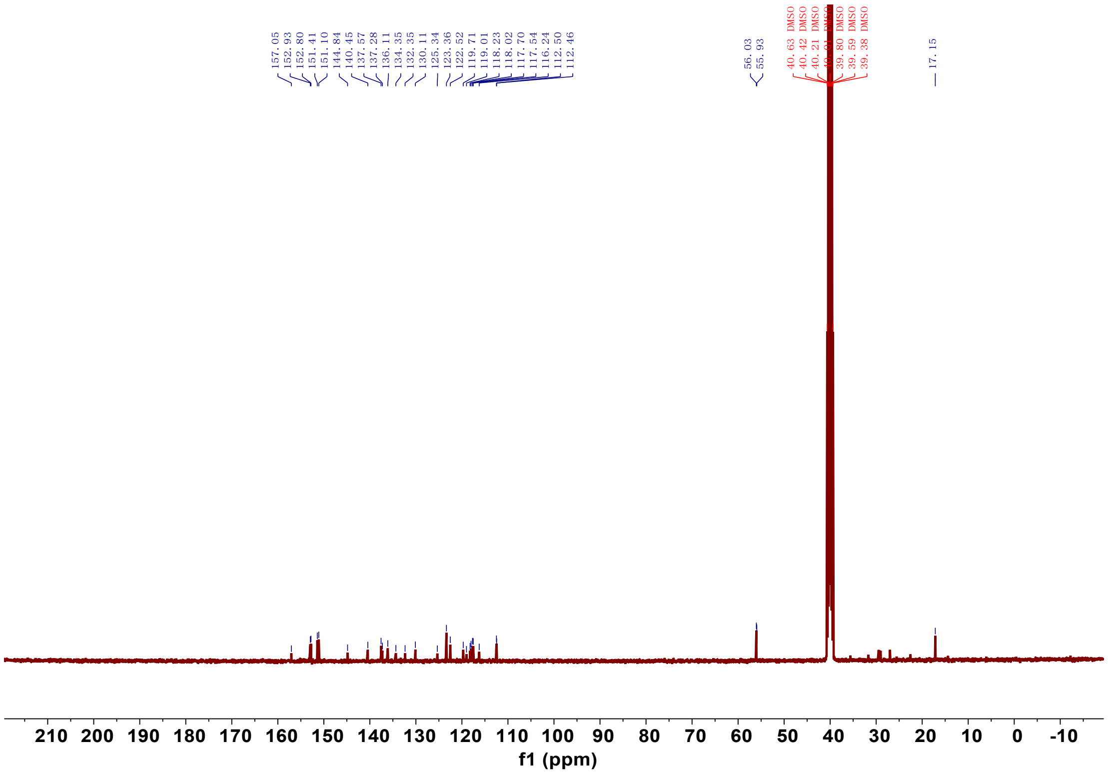

Figure S37. **^{13}C NMR** spectrum of 3,8-HS-OMe-BOD.

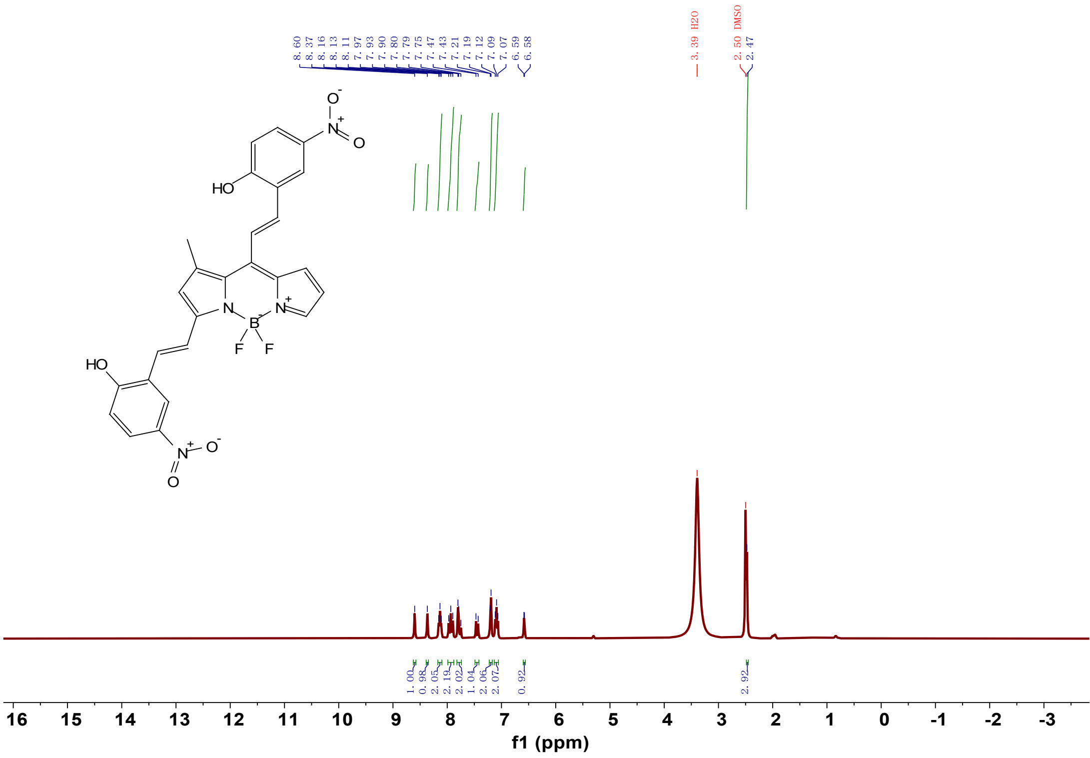

F

igure S38. **^{1}H NMR** spectrum of 3,8-HS-NO_2-BOD.

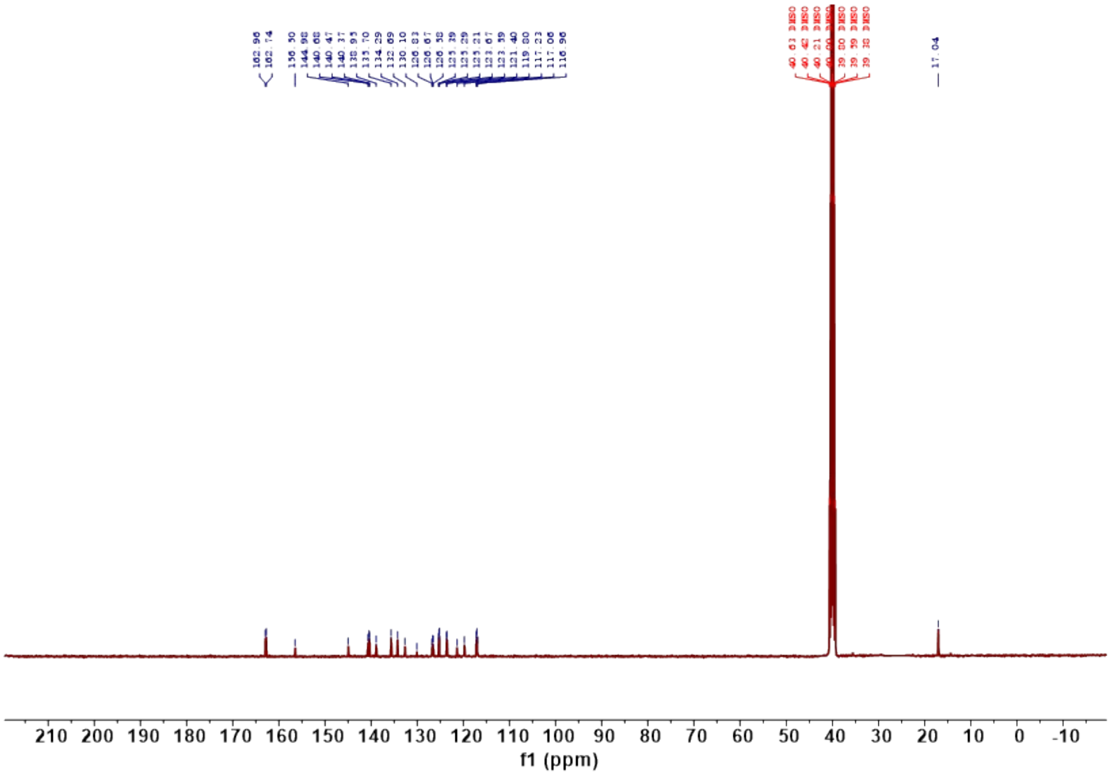

Figure S39. **^{13}C NMR** spectrum of 3,8-HS-NO_2-BOD.

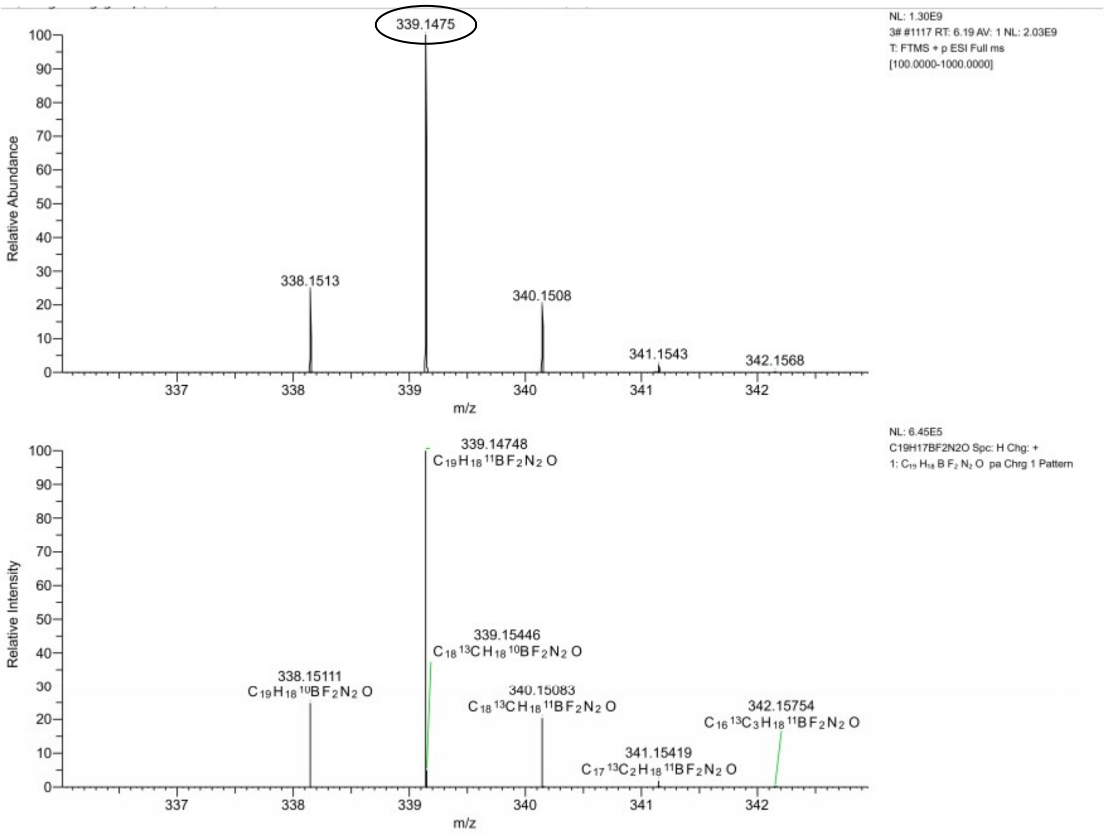

Figure S40. The high-resolution mass spectrometry of 3-HS-BOD.

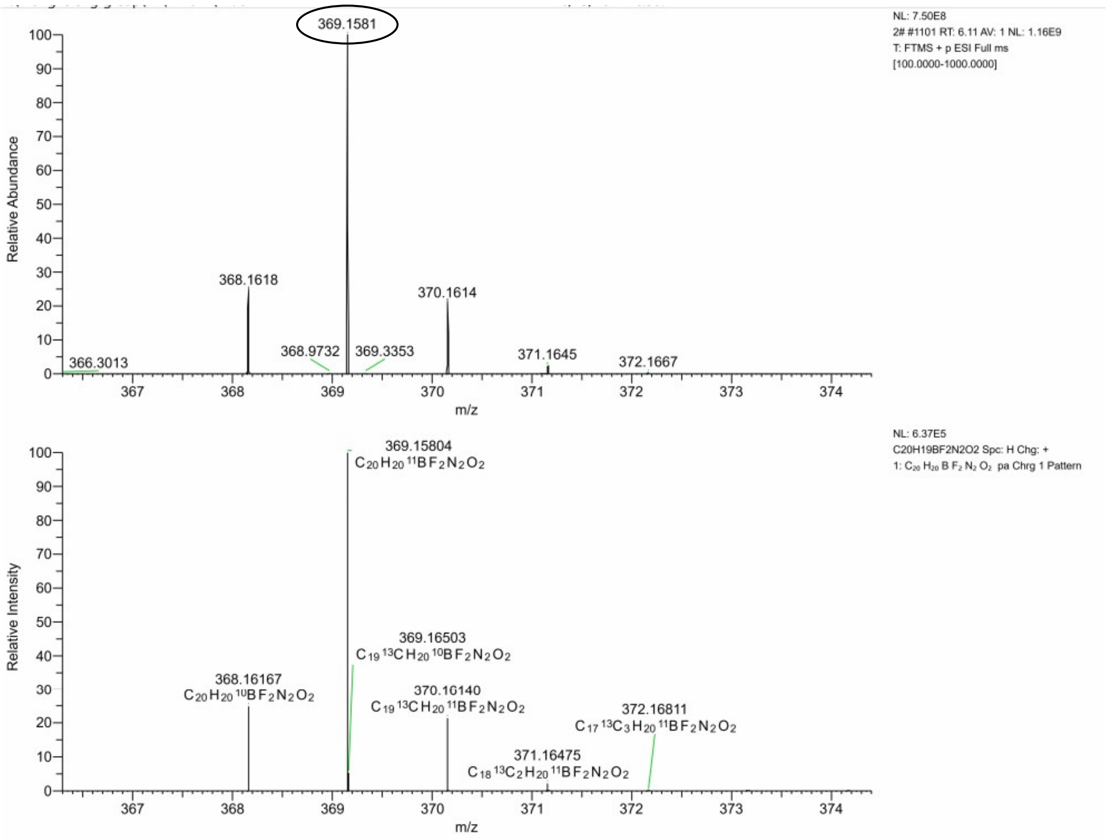

Figure S41. The high-resolution mass spectrometry of 3-HS-OMe-BOD.

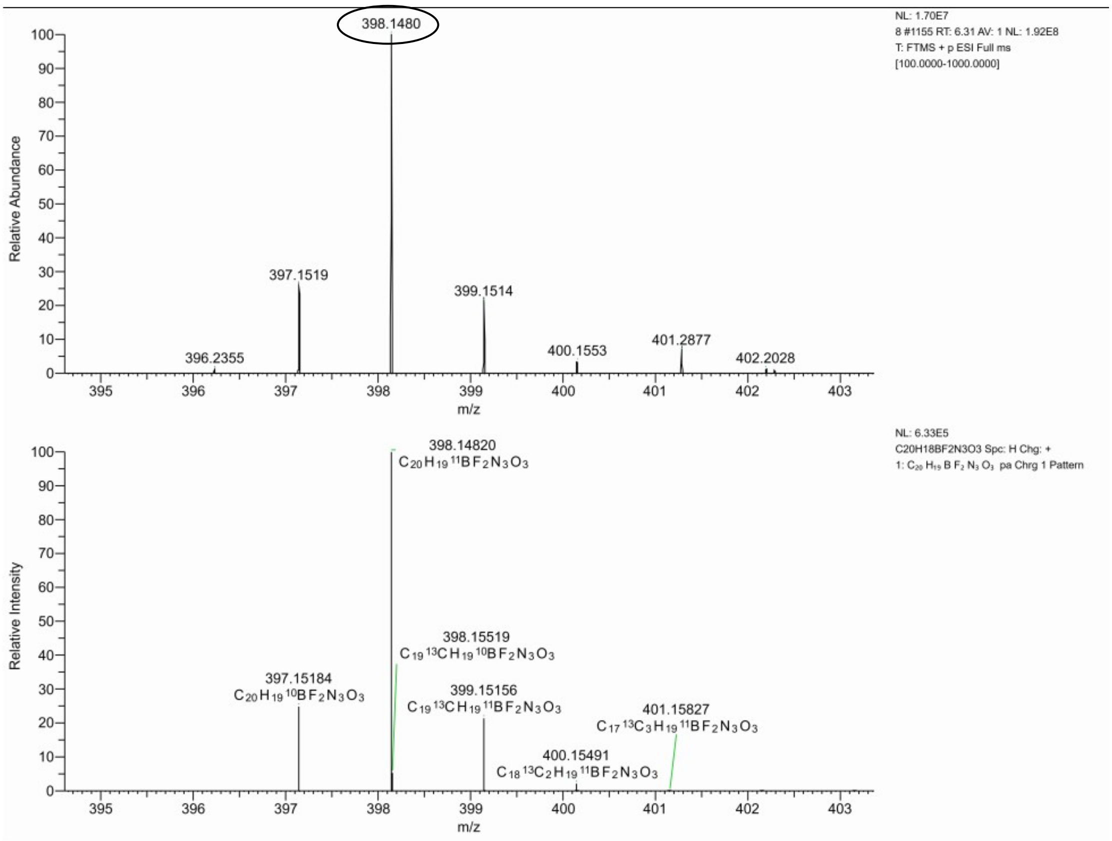

Figure S42. The high-resolution mass spectrometry of 3-HS-NO_2-BOD.

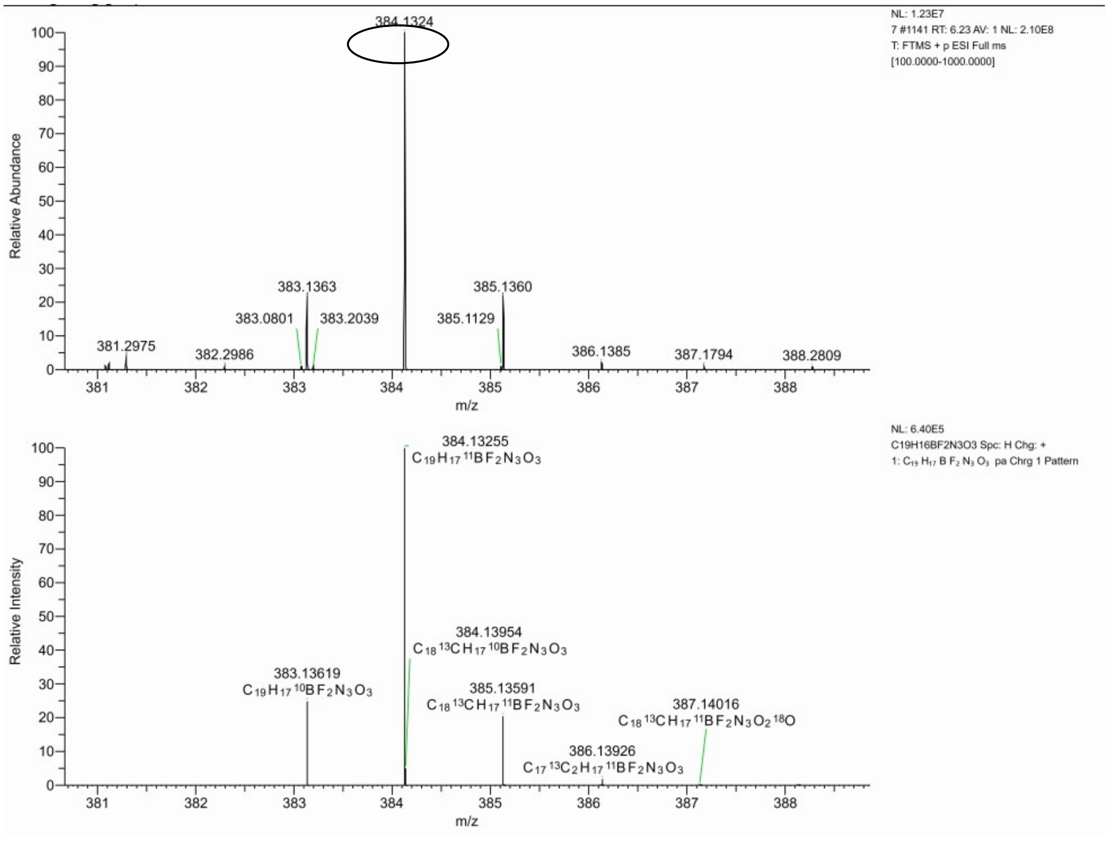

Figure S43. The high-resolution mass spectrometry of 3-MeOS-NO_2-BOD.

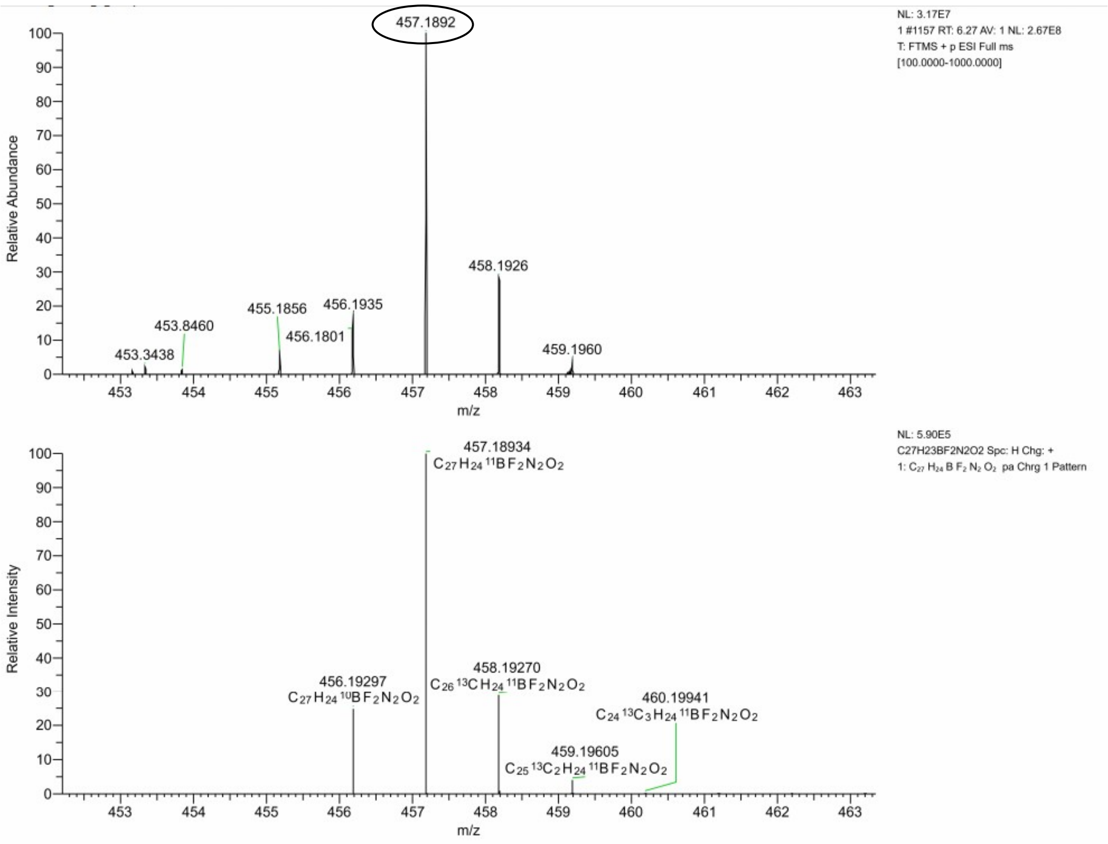

Figure S44. The high-resolution mass spectrometry of 3,5-HS-BOD.

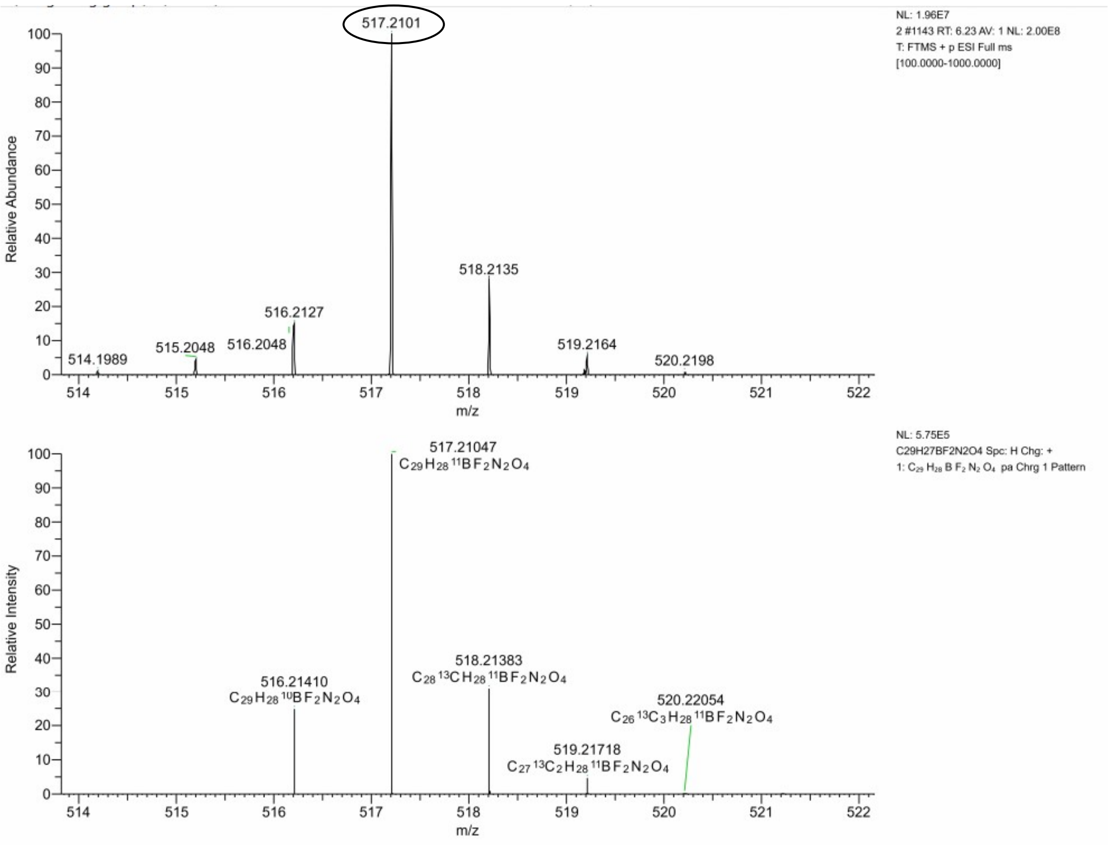

Figure S45. The high-resolution mass spectrometry of 3,5-HS-OMe-BOD.

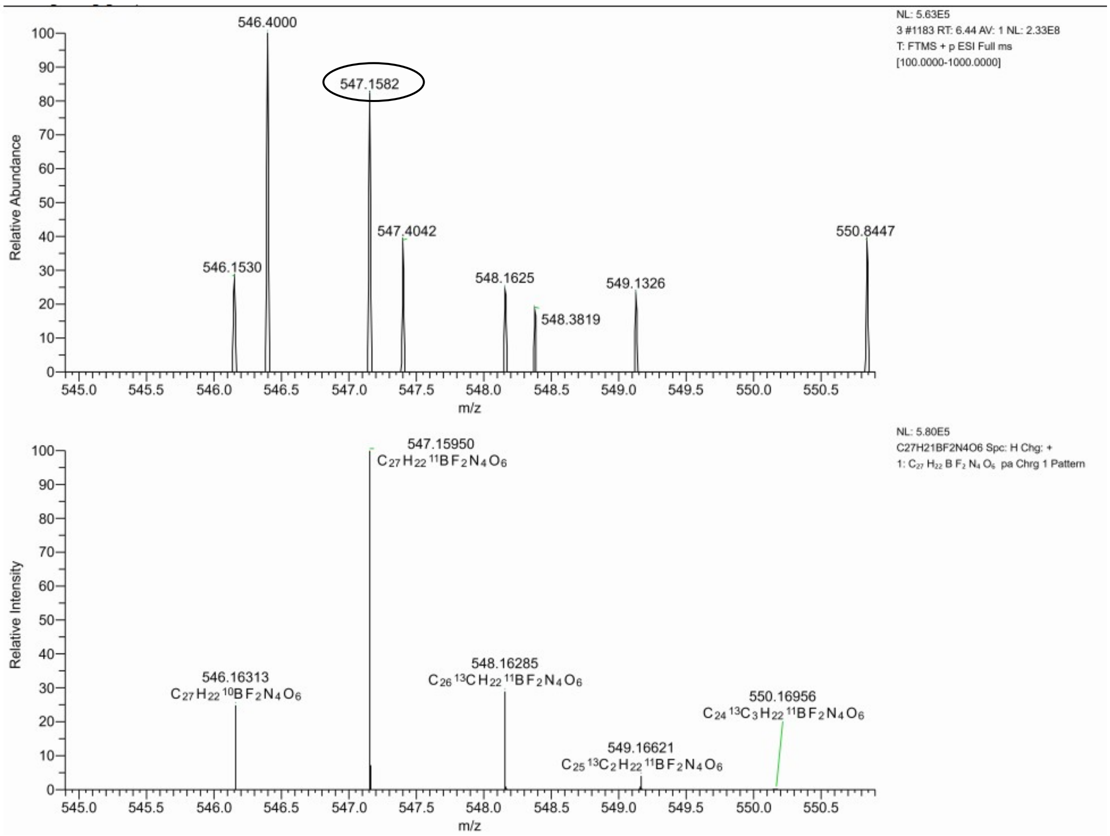

Figure S46. The high-resolution mass spectrometry of 3,5-HS-NO_2-BOD.

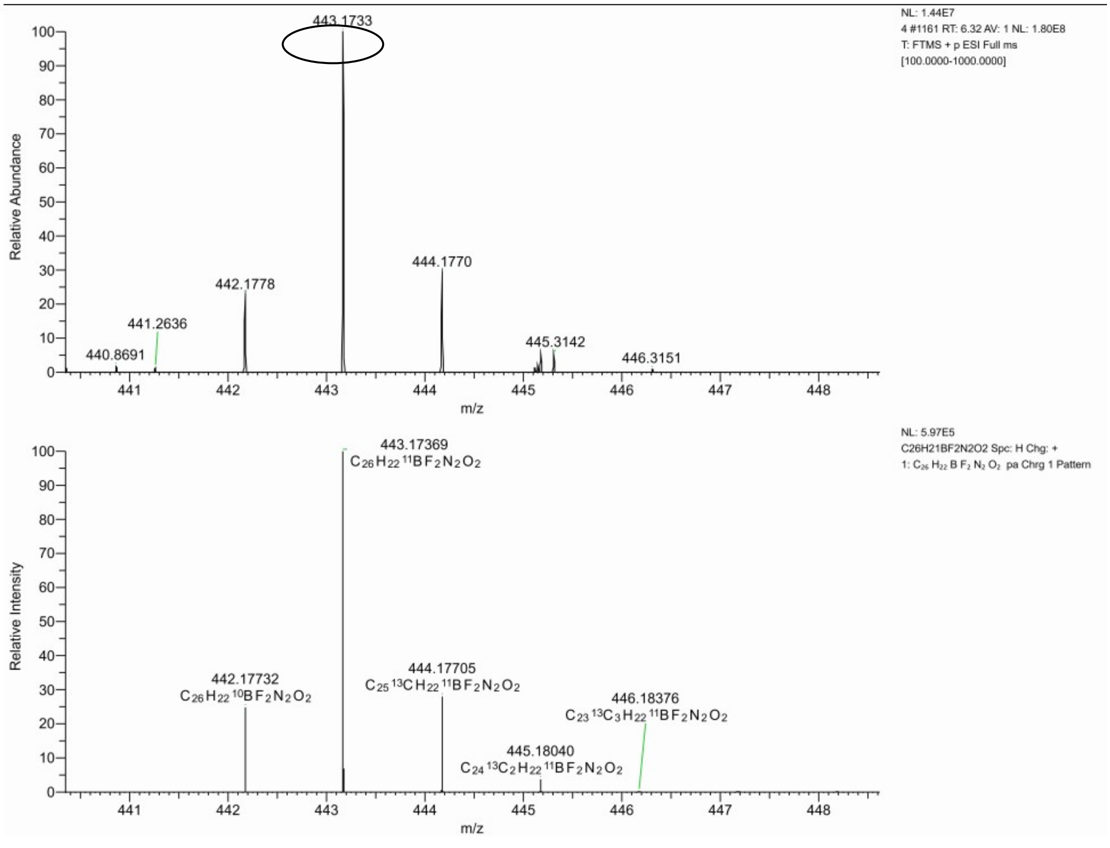

Figure S47. The high-resolution mass spectrometry of 3,8-HS-BOD.

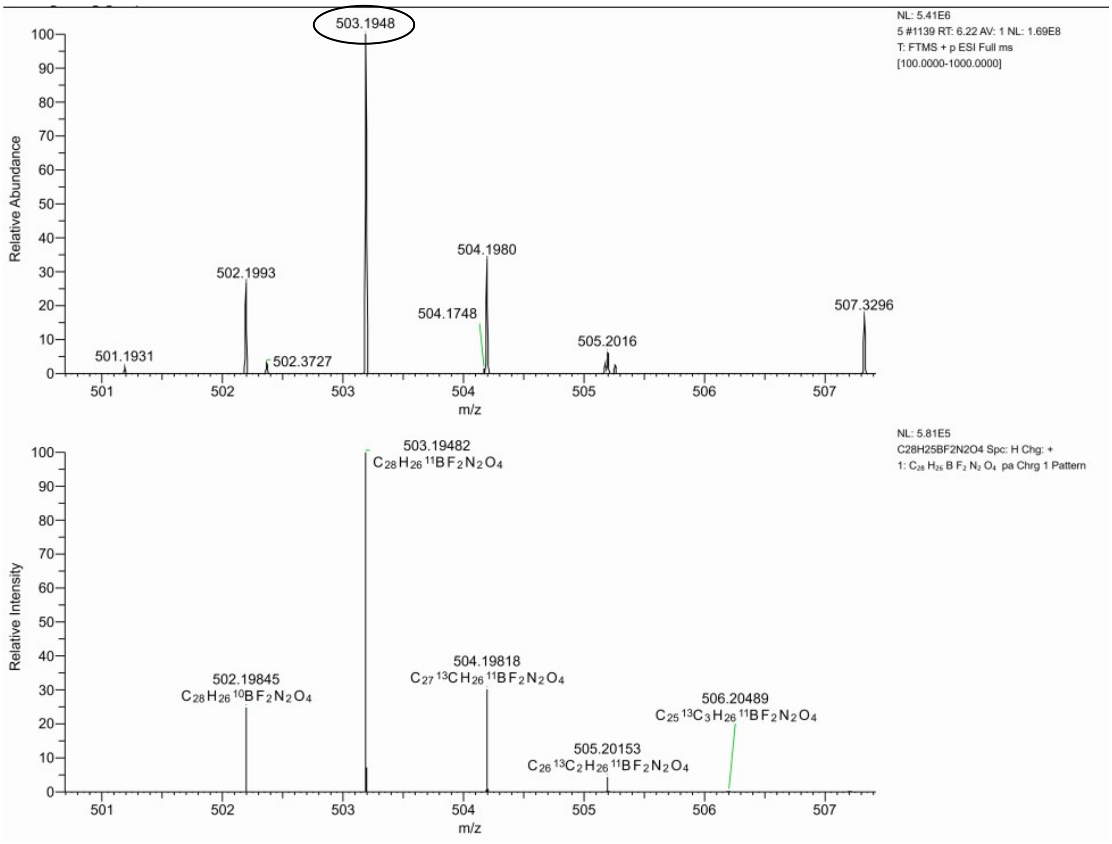

Figure S48. The high-resolution mass spectrometry of 3,8-HS-OMe-BOD.

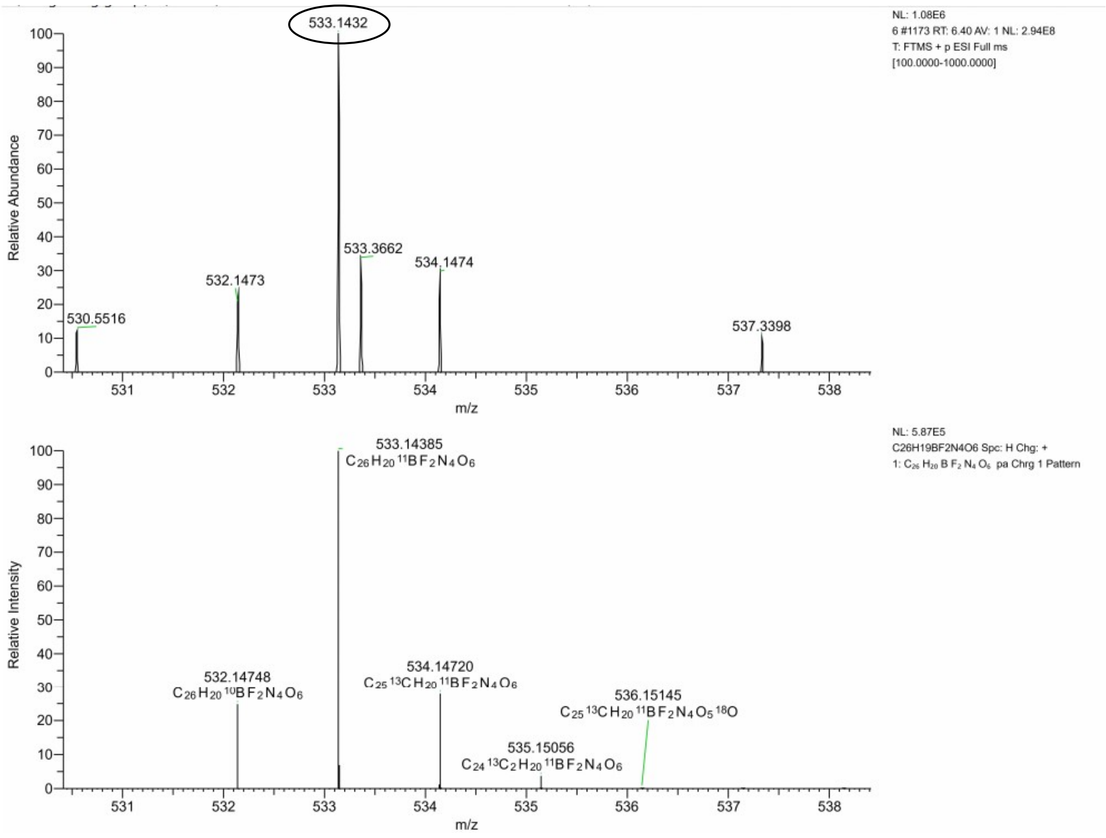

Figure S49. The high-resolution mass spectrometry of 3,8-HS-NO$_2$-BOD.